Published in final edited form as:

Circulation. 2019 November 26; 140(22): 1820–1833. doi:10.1161/CIRCULATIONAHA.119.040740.

Cardiomyocyte HIPK2 Maintains Basal Cardiac Function via ERK Signaling

Yuanjun Guo, BM[1,2], **Jennifer Y. Sui, BA**[1], **Kyungsoo Kim, PhD**[3], **Zhentao Zhang, PhD**[1,4,5], **Xiaoyan A. Qu, PhD**[6], **Young-Jae Nam, MD, PhD**[1,4,5], **Robert N. Willette, PhD**[7], **Joey V. Barnett, PhD**[2], **Bjorn C. Knollmann, MD, PhD**[3], **Thomas Force, MD**[1], **Hind Lal, PhD**[1,8,$]

[1]Division of Cardiovascular Medicine, Vanderbilt University Medical Center, Nashville, TN, USA.

[2]Department of Pharmacology, Vanderbilt University School of Medicine, Nashville, TN, USA.

[3]Division of Clinical Pharmacology, Vanderbilt University Medical Center, Nashville, TN, USA.

[4]Department of Cell and Developmental Biology, Vanderbilt University, Nashville, TN, USA.

[5]Vanderbilt Center for Stem Cell Biology, Vanderbilt University, Nashville, TN, USA.

[6]PAREXEL International, Research Triangle Park, Durham, NC, USA.

[7]Heart Failure Discovery Performance Unit, Metabolic Pathways and Cardiovascular Therapeutic Area GlaxoSmithKline, King of Prussia, PA, USA.

[8]Division of Cardiovascular Disease, UAB | The University of Alabama at Birmingham, Birmingham, AL 35294-1913

Abstract

Background: Cardiac kinases play a critical role in the development of heart failure, and represent potential tractable therapeutic targets. However, only a very small fraction of the cardiac kinome has been investigated. To identify novel cardiac kinases involved in heart failure, we employed an integrated transcriptomics and bioinformatics analysis and identified Homeodomain-Interacting Protein Kinase 2 (HIPK2) as a novel candidate kinase. The role of HIPK2 in cardiac biology is unknown.

Methods: We used the Expression2Kinase algorithm for the screening of kinase targets. To determine the role of HIPK2 in the heart, we generated cardiomyocyte-specific HIPK2 knockout (CM-KO) and heterozygous (CM-Het) mice. Heart function was examined by echocardiography and related cellular and molecular mechanisms were examined. Adeno-associated virus serotype 9 (AAV9) carrying cardiac-specific constitutively active MEK1 (TnT-MEK1-CA) were administrated to rescue cardiac dysfunction in CM-KOs.

[$]**Corresponding authors: Hind Lal, Ph.D.**, Associate Professor of Medicine, Division of Cardiovascular Disease, UAB | The University of Alabama at Birmingham, 1720 2nd Ave South, Birmingham, AL 35294-1913, Tel: 205.996.4219, Fax: 205.975.5104, hindlal@uabmc.edu.

Disclosures

YG, JS, KK, ZZ, YN, JVB, BCK, TF and HL have no conflicting interests to disclose in relation to this work. BW was employed by GSK Pharmaceuticals at the time this work was conducted. XAQ is a former employee of GlaxoSmithKline during the term of this research project and may own GlaxoSmithKline stock. XQA is an employee of PAREXEL International.

Results: To our knowledge, this is the first study to define the role of HIPK2 in cardiac biology. Using multiple HIPK2 loss-of-function mouse models, we demonstrated that reduction of HIPK2 in cardiomyocytes leads to cardiac dysfunction—suggesting a causal role in heart failure. Importantly, cardiac dysfunction in HIPK2 KOs developed with advancing age, but not during development. In addition, CM-KO and CM-Het exhibited a gene dose-response relationship of cardiomyocyte HIPK2 on heart function. HIPK2 expression in the heart was significantly reduced in human end-stage ischemic cardiomyopathy compared to non-failing myocardium, suggesting a clinical relevance of HIPK2 in cardiac biology. *In vitro* studies with neonatal rat ventricular cardiomyocytes corroborated the *in vivo* findings. Specifically, adenovirus-mediated overexpression of HIPK2 suppressed the expression of heart failure markers, *NPPA* and *NPPB*, at basal condition and abolished phenylephrine-induced pathological gene expression. An array of mechanistic studies revealed impaired ERK1/2 signaling in HIPK2 deficient hearts. *In vivo* rescue experiment with AAV9 TnT-MEK1-CA nearly abolished the detrimental phenotype of KOs suggesting that impaired ERK signaling mediated apoptosis as the key factor driving the detrimental phenotype in CM-KO hearts.

Conclusions: Taken together, these findings suggest that cardiomyocyte HIPK2 is required to maintain normal cardiac function via ERK signaling.

Keywords

HIPK2; heart failure; ERK signaling; cardiac function; AAV9

Introduction

Heart failure is a prevalent, costly and growing cause of morbidity and mortality worldwide.[1] Currently, approved pharmacologic therapies for chronic heart failure provide incremental improvements to delay disease progression by reducing cardiac stress through neurohormonal inhibition, volume reduction and vasodilation. To improve clinical outcomes and avoid hemodynamic liabilities, new therapies to target intrinsic cardiac mechanism are urgently needed.

Protein kinases act as key signaling molecules that transduct molecular signals and dynamically modulate various cellular processes. In the heart, they also play a role in cardiac adaptation to stress, as well as, in the progression of heart failure. The human kinome was first described in 2002 and it represents 518 putative protein kinase genes in the human genome[2] and 510 orthologs in the mouse.[3] A comparatively recent study has described cardiomyocyte kinome and kinase expression profile in failing human hearts.[4] This systematic analysis of the cardiac kinome identified several hundred protein kinases in cardiomyocytes (CMs). To date, the studies of cardiac kinome and its role in cardiac pathophysiology have been limited to very few kinase families, such as MAPKs, PI3K, AKT, PKC, and GSK3.[5,6] and have neglected detailed analysis of the majority of highly expressed cardiac kinases. Since protein kinases are often highly tractable and precedented drug targets, it is important to expand our understanding of the cardiac kinome as a means of exploring potential therapeutic opportunities to address the most pressing unmet medical needs in heart failure.

In order to identify novel cardiac kinases potentially involved in heart failure development, we employed an integrated transcriptome and bioinformatics approach (Expression2Kinases (X2K)[7]) using control and failing mouse hearts. Unlike conventional transcriptome screenings, this approach links upstream regulator kinases with the global pattern of observed gene expression via transcription factors to predict potential key regulators of disease progression and potential therapeutic targets.[8] By employing this approach, we identified an unexplored cardiac kinase in the context of cardiac function and dysfunction—HIPK2.

HIPK2 is a conserved serine/threonine and tyrosine nuclear kinase[9] that was discovered as a transcriptional corepressor of NK homeoproteins.[10] Genetic approaches with diverse cell types and organisms have consistently shown that HIPK2 can modulate numerous signaling pathways including TGFβ,[11] Wnt,[12] p53,[13,14] JAK/STAT, NRF2[15] and JNK[16,17] signaling.[18] The pleiotropic function of HIPK2 includes regulation of transcription factors, fibrosis, apoptosis, proliferation, development, and the DNA damage response.[18–20] Although a previous study has implicated HIPK2 as a target of mir-222 in the heart,[21] the role of HIPK2 in the cardiac context has never been studied.

The present study identified HIPK2 as a novel regulator of heart failure progression. We hypothesized and experimentally confirmed that this previously unknown kinase in the heart is critical to maintain basal cardiac function. Cardiomyocyte-specific deletion of HIPK2 leads to progressive deterioration of cardiac function with age. Consistent with these findings in mouse models, we observed that human failing hearts are associated with significantly reduced expression of HIPK2. At the molecular level, we show that HIPK2 deficiency leads to enhanced apoptosis via decreased ERK1/2 phosphorylation, which eventually results in attenuated cardiac function.

Methods

Data availability

The data that support the findings of this study are available from the corresponding author upon reasonable request. Microarray data are available at the GEO repository (GSE136308). Detailed materials and methods are available in the online Supplemental Material.

Animals generation and breeding

The HIPK2 global knockout (KO) mice were a generous gift from Dr. Eric Huang, UCSF.[22] The global KO mice were maintained in 129 and B6 mixed background. C57BL/6NTac-Hipk2$^{tm2a(EUCOMM)Hmgu}$/Cnrm mice (EM:05113) were purchased from the European Mouse Mutant Archive (EMMA).[23] B6.129S4-*Gt(ROSA)26Sor*$^{tm1(FLP1)Dym}$/RainJ (stock# 009086)[24] and B6.FVB-Tg(Myh6-cre)2182Mds/J mice (stock# 011038)[25] were purchased from the Jackson Laboratory. Generation of the cardiomyocyte-specific HIPK2 KO mice is described in the results. C57BL/6J mice used in this study were purchased from the Jackson Laboratory (stock #000664). The Institutional Animal Care and Use Committee of Vanderbilt University Medical Center approved all animal procedures and treatments

(protocol # M1700133–00). All animals were housed in a temperature-controlled room with a 12:12h light-dark cycle and received humane care.

AAV9 virus construction and administration

pMCL-HA-MAPKK1-R4F [delta(31–51)/S218E/S222D] (MEK1-CA) plasmid was a gift from Natalie Ahn (Addgene plasmid #40810; http://n2t.net/addgene:40810; RRID: Addgene_40810). MEK1-CA plasmid was cloned into a pre-made AAV9 generating plasmid with Troponin (TnT) promoter (VectorBuilder #VB180411–1135acz) to make the TnT-MEK1-CA plasmid. The TnT-MEK1-CA plasmid was then packaged into AAV9 virus (Vigene Biosciences, Inc.). AAV9 virus was delivered by tail vein injection or jugular vein injection.[26] Briefly, mice were anesthetized by Xylazine/Ketamine. A 1-cm cut was made above the right clavicle, and then the jugular vein was exposed. The virus was diluted by 0.9% saline to 250μl and slowly delivered into the jugular vein.

Statistics

Differences between data groups were evaluated for significance with the use of the nonparametric Mann-Whitney test or Student's t-test for comparison between two groups, and Analysis of Variance (ANOVA) or mixed-effects analysis with Turkey's post hoc test for comparison among more than two groups. (GraphPad Prism Software Inc, San Diego, CA). Data are presented as mean±SEM unless noted otherwise. For all tests, a P value < 0.05 was considered to denote statistical significance.

Results

Identification and Characterization of HIPK2 in Failing Hearts

Considering the essential role of cardiac kinases in disease progression and their general tractability as drug targets, we employed a bioinformatics approach (Expression2Kinase)[7] to identify kinase regulators involved in heart failure progression (Figure 1A). C57BL/6 male mice were subjected to transaortic constriction (TAC) to induce heart failure or sham surgery. At 6 weeks post-TAC, RNA samples from the left ventricle were subjected to microarray analysis. We first identified the differentially expressed genes (FC≥1.5, adjusted $p<0.01$) in TAC versus sham hearts. Secondly, we postulated transcription factors (TFs) of those differentially expressed genes using three algorithms: Ingenuity Pathway Analysis (IPA, Qiagen), Position Weight Matrix (PWM), and ChIP Enrichment Analysis (ChEA).[7] With the IPA approach, a total of 40 associated transcription factors were identified. These transcription factors were responsible for 27 up-regulated genes, and 13 down-regulated genes (Supplemental Figure 1A). We also predicted responsible TFs for the observed gene expression changes using two additional approaches: 1) ChEA, based on chromatin-protein binding, and 2) TransFac and Jasper analysis, based on specific promotor binding (PWM) (Supplemental Figure 1B). Thus, these three approaches to predict the responsible TFs generated three distinct lists of TFs for further analysis. Thirdly, we linked these TFs with potential upstream kinase regulators by constructing a protein-protein interaction network.[27] We then performed a Kinase Enrichment Analysis[28] on those proteins interacting with predicted TFs, and identified the top 25 "extrapolated" kinase regulators of each TF prediction approach (Figure 1A). Even though predicted by distinct approaches, 52% kinase

targets (in red) were common in three kinase lists and 70% (in blue) were common in two lists. Furthermore, these three lists were highly dominated by commonly described kinases known for their indispensable role in cardiac biology (e.g. AKT, GSK3, and MAPKs). The identification of these "positive control" kinases was also a validation of this analytical approach. Among those candidates, we identified a potential modulator of heart failure—HIPK2, a kinase whose role in cardiac biology has never been studied before. To determine the role of HIPK2 in failing human hearts, we examined the expression of HIPK2 in heart tissue from patients with end-stage ischemic cardiomyopathy. The expression of HIPK2 was dramatically decreased in failing hearts compared with normal human hearts (Figure 1B).

Global KO of HIPK2 Leads to Decreased Cardiac Function

To evaluate the cardiac function of HIPK2, we first examined HIPK2 global knockout (KO) mice[22] by echocardiography. At 2 months of age, heart function of wildtype (WT) and KO was comparable (Supplemental Figure 2A–2F). However, HIPK2 KO mice developed cardiac dysfunction at around 5 months of age, reflected by significantly decreased Ejection Fraction (EF) and Fractional Shortening (FS) (Figure 2A and 2B). There was no significant change in left ventricle dimension and posterior wall thickness (Figure 2C–2F). We also examined the contractility and calcium handling in single isolated adult CMs at the same age. Surprisingly, there was no significant change in the KO versus WT (Supplemental Figure 3A–3R). The intact contractility and calcium handling in HIPK2-deficient cardiomyocytes suggest a minimal to no role of these processes in observed detrimental phenotype in KO hearts. The heart weight of KOs, as well as the heart weight normalized by the tibia length, was significantly decreased compared to WT (Figure 2G and 2H). It is important to note that the body weight of KOs was significantly less than that of the littermate controls (Figure 2I). Further examination of the body mass composition using the Nuclear Magnetic Resonance analyzer revealed that the decreased body weight was mainly due to a lower percentage of fat mass in KOs (Figure 2J), which is consistent with previous findings.[29]

Generation and Characterization of Cardiomyocyte-Specific HIPK2 KO Mice

HIPK2 global KO mice are known to have a defective fat development phenotype that accounts for significantly reduced body weight of KOs in comparison to littermate controls. Of note, body weight is a prominent confounding factor of cardiac function. Furthermore, global gene deletion can lead to compensatory effects that may further complicate the interpretation of phenotypes. Indeed, the HIPK2 global KO mouse displays several defects in various systems.[11,29–32] All these factors limit the use of this global KO mouse model to further study the role of HIPK2 in the heart. Thus, in order to examine the role of HIPK2 in cardiac biology, we generated cardiomyocyte-specific HIPK2 KO mice. The C57BL/6NTac-Hipk2$^{tm2a(EUCOMM)Hmgu}$/Cnrm mouse (HIPK2^{tm2a}) was obtained from the European Mouse Mutant Archive (EMMA)[23] and crossed with B6.129S4-*Gt(ROSA)26Sor*$^{tm1(FLP1)Dym}$/RainJ[24] (FLP) mice to generate mice with the *HIPK2 flox* allele. Thereafter, *HIPK2 flox* mice were mated with mice expressing αMHC promoter-driven Cre to achieve the cardiomyocyte-specific HIPK2 KO mice (HIPK2$^{flox/floxCre+/}$, CM-KO), heterozygous mice (HIPK2$^{flox/Cre+/}$, CM-Het) and littermate controls (HIPK2$^{flox/flox}$, Control) (Figure 3A, Supplemental Figure 4A). αMHC-Cre expression led to about 87%

reduction of HIPK2 expression in CM-KO hearts (Figure 3B). As expected, heterozygous hearts demonstrated about 50% reduction of HIPK2 compared with Control hearts (Figure 3C). Importantly, the body weight of CM-KO and Control mice was comparable (Supplemental Figure 4B).

CM-Specific Deletion of HIPK2 Leads to Cardiac Dysfunction

To determine the cardiac phenotype of CM-KO mice, CM-KO and Control mice were examined by echocardiography. At 2 months of age, CM-KOs and Controls had comparable heart function (Figure 4A and 4B), suggesting the absence of any developmental cardiac defects. Intriguingly, at 3 months of age, the EF and FS of CM-KO mice were significantly decreased in comparison to their littermate controls (Figure 4A–4C). Consistent with deteriorating cardiac function, the internal dimension of KO hearts had a trend of dilation, yet not significantly different from the control at this age (Figure 4C–4G). The mRNA expression of heart failure markers *NPPA* and *NPPB* was significantly elevated, as was the *MYH7* and the *MYH6/MYH7* ratio, which all indicate LV failure (Figure 4H). There was no significant change in heart weight normalized by tibia length (Supplemental Figure 5A) and CMs cross-sectional area (Supplemental Figure 5B–5C) in CM-KO mice compared with Controls. To further assess the change in cell growth, we isolated adult CMs from CM-KOs and Controls at 3 months of age and measured cell volume using Imaris.[33] The cell volume and the length/width ratio were consistently comparable between CM-KO and Control mice (Supplemental Figure 6A–6C). Since HIPK2 is known for its function in regulating fibrosis and fibroblasts,[34] we evaluated the mRNA expression of pro-fibrotic genes *COL1A1* and *COL1A2*. The gene expression was comparable between the CM-KO and Control (Supplemental Figure 6D). We also did not observe significant fibrosis deposition in Masson's trichrome stained CM-KOs heart sections (Supplemental Figure 5B). This suggests that CM HIPK2 is not a key regulator of myocardial fibrosis, and thus, this excludes the driving role of fibrosis in the pathogenesis of heart failure in CM-KO hearts. Since calcium handling is key to the LV function, we further examined the contractility and calcium handling in the isolated adult CMs. Surprisingly, all parameters of contractility and calcium handling were comparable between CM-KOs and Controls at both basal (Supplemental Figure 7A–7I) and isoproterenol-stimulated conditions (Supplemental Figure 7J–7R). This indicates that loss of HIPK2 does not affect single cell contractility and calcium handling, eliminating these factors as contributors to the cardiac dysfunction in CM-KOs. At 8 months of age, the heart failure much worsened with the disease progression as reflected by a dramatic decrease in EF and FS (Figure 4I–4K). Consistently, the CM KO heart also gradually developed dilatative remodeling with significantly enlarged LV internal diameter, thinner posterior wall, increased heart weight, cell surface area and fibrosis deposition (Figure 4L–4S).

To further delineate the role of HIPK2 in the cardiomyocyte, we employed a cell culture model of neonatal rat ventricular cardiomyocytes (NRVMs). NRVMs were infected with adenovirus carrying shRNA-HIPK2 (Ad-shRNA-HIPK2) or shRNA-scrambled (Ad-scrambled) for 48 hours, and reactivation of the fetal gene program was examined. The suppression of HIPK2 in NRVMs resulted in significant elevation of *NPPA* (Figure 4T), which is consistent with the phenotype in CM-KOs. As a gain-of-function approach, we

infected NRVMs with adenovirus expressing WT HIPK2 (Ad-HIPK2) or LacZ (Ad-LacZ). Adenovirus-mediated overexpression of HIPK2 suppressed the *NPPA* and *NPPB* expression at the basal condition (Supplemental Figure 8A–8B). Strikingly, the phenylephrine-induced elevation of *NPPA* and *NPPB* was completely abolished by overexpression of HIPK2 (Supplemental Figure 8A–8B). Overexpression or knockdown of HIPK2 does not alter the cardiomyocyte cell surface area (Supplemental Figure 9A and 9B). This finding is consistent with the phenotype we observed *in vivo* as well as with the literature.[21] Overall, these *in vitro* results are consistent with the detrimental phenotype of HIPK2 CM-KO hearts and also suggest a cardioprotective role of HIPK2.

The findings above also showed that cardiac dysfunction of two KO models, the CM-KO as well as the global KO, both developed in adulthood (after 2-month-old). This is despite that αMHC-driven deletion occurs as early as at birth and the global KO mice lack gene activity throughout embryogenesis. This suggests the hypothesis that HIPK2 expression is age-related and may dominate in the fully mature heart. To examine the HIPK2 expression at different ages, we harvested hearts from C57BL/6J mice at E12.5, day 1, and 4-month-old, representing embryonal, neonatal and adult stages respectively. Analysis of HIPK2 expression reveals a higher HIPK2 expression level in adults compared to embryonic or neonatal hearts (Figure 4U). This expression pattern may partially explain the time course of the cardiac phenotype we observed in both KO models.

CM-Specific HIPK2 Haploinsufficiency is Sufficient to Induce an Adverse Cardiac Phenotype

To determine if the level of HIPK2 gene expression in the heart directly corresponds to function, we compared CM-Het to the littermate control. Cardiac function was comparable between the CM-Het and Control up to 3 months of age. However, the heart function of CM-Hets gradually decreased after 3 months and was significantly reduced at 6 months of age as reflected by significantly decreased EF and FS (Figure 5A and 5B). As discussed above, the CM-KOs demonstrated marked cardiac dysfunction much earlier—at 3 months of age. Thus, these findings indicate a direct relationship between the level of cardiomyocyte HIPK2 expression and cardiac function. CM-Het mice also exhibited left ventricular dilation and thinning of the left ventricular wall (Figure 5C–5F). At the molecular level, the expression of the heart failure marker *NPPA* was elevated by about 10-fold in the Het heart (Figure 5I). Comparable fibrosis in CM-Het and Control hearts indicated that cardiomyocyte-specific dysfunction preceded the development of fibrosis in the HIPK2 deficient hearts (Supplemental Figure 10).

HIPK2 Facilitates its Cardioprotective Effects through ERK Signaling

We next explored the potential molecular mechanism of the development of cardiac dysfunction in HIPK2 deficient hearts. It is well accepted that analysis of heterozygote animals is a more physiologically relevant strategy compared to that of homozygous KO. Considering this, we used 6-month-old Het null heart tissue for the molecular mechanistic studies. As there is no literature regarding HIPK2 and cardiac function, we chose to examine major pathways implicated in myocardial function and dysfunction[5] in the setting of HIPK2 deficiency. Many of these cardiac pathways were either not significantly changed or the

nature of the change was not consistent with the observed phenotype (Supplemental Figure 11). Importantly, however, we discovered that ERK1/2 phosphorylation was significantly decreased in the CM-Het mouse heart (Figure 6A–6C). It is well established that ERK is essential to maintain cardiac function, as mice with cardiac-specific deletion of ERK1/2 leads to spontaneous cardiac dysfunction and heart failure.[35]

Further mechanistic studies to examine HIPK2 regulation of ERK were performed *in vitro* using NRVMs. For the loss-of-function approach, NRVMs were infected with ad-shRNA-HIPK2 or ad-scrambled, and cell lysates were analyzed for the phosphorylation of ERK. As expected, knockdown of HIPK2 significantly decreased both ERK1 and ERK2 phosphorylation (Figure 6D–6F). As a gain-of-function strategy, NRVMs were infected with Ad-HIPK2 or Ad-LacZ and cell lysates were analyzed to examine the ERK phosphorylation (Figure 6G–6I). In contrast to the loss-of-function approach, overexpression of HIPK2 leads to significant elevation of ERK1/2 phosphorylation. Since the function of HIPK2 could be dependent on its kinase domain or protein-protein interaction with other domains,[36,37] to examine the requirement of HIPK2 kinase function in ERK phosphorylation, we infected NRVMs with HIPK2 kinase-dead (K221A) adenovirus (Ad-HIPK2-KD). Interestingly, ad-HIPK2-KD did not affect ERK phosphorylation, which indicates that the regulation of ERK by HIPK2 is kinase-dependent (Figure 6J). Furthermore, in contrast to HIPK2 overexpression, kinase-dead mutation of HIPK2 failed to display any cardioprotective effect (Figure 6J and 6K). This indicates that the regulation of ERK and cardiac function by HIPK2 is kinase-dependent. Taken together, these findings suggest that HIPK2 is critical to myocardial ERK signaling which, in turn, is vital to the maintenance of basal cardiac function.

Loss of HIPK2 in Cardiomyocytes Promotes Apoptosis

It is well established that ERK signaling protects the heart from stress-induced apoptosis,[38] a key driver of cardiac remodeling and heart failure.[39] HIPK2 is also known as a key regulator of apoptosis,[40] though its function in this process is complex and context-dependent. Therefore, we investigated the extent of cardiomyocyte death and underlying mechanism in our model. We first assessed the proapoptotic and anti-apoptotic pathway modulators—BAX and BCL-XL by Western blot analysis in 3-month-old LV tissue. The expression of proapoptotic molecules BAX was significantly elevated in the CM-KO as was the BAX/BCL-XL ratio (Figure 7A–7D). We confirmed the activation of apoptosis by Terminal deoxynucleotidyl transferase dUTP nick end labeling (TUNEL) assay. There was a significant elevation of TUNEL positive CM nuclei in CM-KO (Figure 7E and 7F). The apoptotic events became more remarkable with the disease progression at 8-month-old (Figure 7G–7L). Since cell apoptosis is highly regulated by mitochondria, we further examined whether mitochondrial dysfunction or energetic dysregulation was altered. To examine the mitochondrial function, we measured the tissue O_2 flux with Orobros Oxygraphy, however, there was no significant change in the CM-KO LV tissue upon addition of different substrates (Supplemental Figure 12). We further assessed the cell O_2 consumption rate by Seahorse in NRVMs with HIPK2 overexpression or knockdown. Consistent with the *in vivo* findings, HIPK2 does not affect mitochondrial function and O_2 consumption (Supplemental Figure 13A and 13B). Therefore, metabolic dysfunction of

cardiomyocytes is not a driver of the cardiac phenotype seen in CM-KOs. Overall, our data clearly implicate impaired ERK signaling, leading to loss of functional cardiomyocytes, as a primary driver of cardiac dysfunction in CM-KOs.

AAV9 TnT-MEK1-CA Rescues the Cardiac Dysfunction of CM-KO mice

Finally, we aimed to determine the molecular mechanism of the observed detrimental phenotype in CM-KO mice, with our hypothesis being that impaired ERK signaling in CM-KO hearts is the primary driver of the observed cardiac dysfunction. To test this hypothesis, we performed an *in vivo* rescue experiment with AAV9-mediated gene therapy system to restore ERK signaling. We used Troponin (TnT)-driven constitutively active MEK1 (MEK1-CA), upstream of ERK, to see whether AAV9 TnT-MEK1-CA can rescue the HIPK2 deficient phenotype by restoring ERK phosphorylation. To generate the AAV9 TnT-MEK1-CA, MEK1-CA plasmid with HA tag[41] was cloned into a pre-made AAV9 TnT plasmid construct, thereafter packaged to AAV9 (Figure 8A). First, we performed a pilot experiment using AAV9 TnT-GFP to test the feasibility of cardiomyocyte-specific gene expression delivered by AAV9 and optimize the appropriate viral dose and route of delivery. To ensure the reliability of AAV9 delivery in C57BJ6 background mice, we compared the jugular vein delivery to the tail vein injection.[26] The dose-dependent expression of GFP in the LV clearly indicated the jugular vein as a comparatively more efficient route for reliable and consistent viral delivery (Supplemental Figure 14A and 14B). Thereafter, we delivered 5×10^{11} GC of AAV9 TnT-MEK1-CA or AAV9 TnT-GFP to 1-month-old CM-KO or Control mice via the jugular vein. Heart function was monitored by serial echocardiography (Figure 8B). The infection efficiency was confirmed by Western blot analysis of GFP and HA (Figure 8C). As expected, the ERK phosphorylation was restored in the CM-KO mice with AAV9 TnT-MEK1-CA administration (Figure 8C-8E). Indeed, AAV9 TnT-MEK1-CA significantly improved the EF and FS of CM-KO so that the cardiac function of CM-KO with MEK1-CA was no longer significantly different from the Control (Figure 8F and 8G, Supplemental Figure 15A–15D). There was no significant change of the normalized heart weight among groups (Supplemental Figure 15F). Histological analysis of heart sections showed a comparable CM cross-sectional area and fibrosis deposition (Supplemental Figure 15E–15G) in the AAV9 groups, consistent with prior observations in CM-KO hearts. The increased proapoptotic pathway—BAX expression and BAX/BCL-XL were also significantly rescued by MEK1-CA injection (Figure 8H-8K). TUNEL staining also consistently showed decreased positive CM nuclei in the rescue group (Figure 8L and Supplemental Figure 15H). Thus, restoring ERK signaling in KOs with MEK1-CA efficiently rescued the aberrant activation of pro-apoptotic signaling, attenuated the ongoing cardiomyocyte death, and thus preserved the cardiac function. These findings strongly validate the hypothesis that impaired ERK signaling is a key mechanism of cardiac dysfunction in HIPK2 CM-KOs.

Discussion

Alarming statistics of human suffering from heart failure and the resultant economic impact necessitate the investigation of new efficient molecular targets to improve preventive and therapeutic strategies. Cardiac kinases are essential molecules in the cardiac pathogenesis as

well as tractable targets for treatment. In the current study, we used the X2K approach to screen kinase targets in a heart failure model and identified a previously unexplored cardiac kinase HIPK2. This is the first study to fully describe the role of HIPK2 in the heart by using both global and cardiomyocyte-specific KO mice in conjunction with a series of *in vitro* studies. We showed that loss of HIPK2 is detrimental to heart function. In addition, we clearly established a dose-dependent effect of the gene level of HIPK2 on cardiac function, as about 50% knockdown of HIPK2 (CM-Het mice) slowed down the progression of heart failure compared to an almost complete loss of HIPK2 (CM-KO mice). This precise dose-dependent effect of HIPK2 level on cardiac function further indicates the functional relevance of HIPK2 in cardiac pathology.

Previous studies indicate that HIPK2 is critical to development and differentiation, such as in neural development,[22,42,43] angiogenesis,[31] and hematopoiesis.[18,32] Our findings indicate that HIPK2 is essential to cardiac function in adults rather than to cardiac development or maturation. The cardiac function of global KO and cardiac-specific KO mice were comparable to their respective controls up to 2 months of age. However, the heart function of KOs quickly deteriorates in adults suggesting the necessity of HIPK2 to maintain adult heart homeostasis. This line of reasoning is further supported by our findings that HIPK2 expression is significantly increased in mature hearts[4]. Taking into account the protection with HIPK2 overexpression in NRVMs and reduced HIPK2 expression in failing human hearts, we speculate that cardiac-specific restoration of HIPK2 in failing hearts may slow down the disease progression. With that said, further studies with cardiac-specific HIPK2 transgenic mice will be required to test this hypothesis.

Mechanistically, we characterized the main cellular processes and signaling pathways involved in cardiac remodeling thoroughly and identified that HIPK2 exerts its cardiac effect primarily through ERK regulated apoptosis. Importantly, this is the first study to identify ERK as a downstream target of HIPK2. Using both gain- and loss-of-function approaches, we clearly demonstrate that HIPK2 is required for cardiac ERK signaling. Furthermore, our studies suggest that impaired ERK signaling in CM-KO is the primary mechanism leading to cardiac dysfunction. This conclusion is strongly supported by our rescue experiment with AAV9-mediated gene therapy to restore ERK signaling, which significantly improved heart function in CM-KOs. Indeed, numerous studies have suggested the essential role of ERK signaling in myocardial pathophysiology.[35,38] Mice with cardiac-specific deletion of ERK1/2 showed spontaneous cardiac dysfunction and chamber dilation leading to severe heart failure and death.[35] Conversely, transgenic mice with cardiac-specific activation of ERK1/2 signaling (via MEK1 expression) augmented cardiac function. Cardiac-specific MEK1 transgenic mice were partially resistant to stress-induced heart failure.[38] Intriguingly, Trametinib, a MEK inhibitor used for the treatment of metastatic melanoma, is also found to decrease heart function.[44] These pieces of evidence suggest that an intact ERK signaling is critical to maintain cardiac homeostasis in humans. Our AAV9 rescue experiment also supports the concept that impaired ERK signaling exerts its detrimental cardiac effects by activating the apoptotic signaling and cardiomyocyte death. The continuous loss of functional CMs in KO hearts could also explain the disagreement that KOs maintained the normal contractility and calcium handling at the cellular level, while the contractile function decreased at the organ level.[45,46]

Overall, this study identifies HIPK2 as a critical regulator of cardiac homeostasis. Cardiac-specific deletion of HIPK2 leads to impaired ERK signaling and cardiac dysfunction. This pathway is central to the pathology because a rescue experiment to restore ERK signaling abolished the cardiac dysfunction phenotype in CM-KOs. We also identified that HIPK2 is downregulated in the myocardium of heart failure patients. Clinically, inhibition of HIPK2 has been proposed as a therapeutic approach for the management of renal fibrosis and certain cancers.[18,47] Our current data provide a cautionary note for the potential adverse consequences of genetic or pharmacological HIPK2 inhibition in the adult heart.

Supplementary Material

Refer to Web version on PubMed Central for supplementary material.

Acknowledgments

The authors would like to thank Dr. Joshua Fessel and Christi Moore in Division of Allergy, Pulmonary, and Critical Care, Department of Medicine, Vanderbilt University Medical Center for the guidance and support for the Oroboro Oxygraph and Seahorse study. We would like to thank Kaylen Kor for the adult CMs isolation, Dr. Zhizhang Wang and Dr. Lin Zhong for Echocardiographic examination. The authors would like to acknowledge the Vanderbilt Cardiology Core lab for Translational and Clinical Research for their technical assistance and coordinating the specimen biorepository. All histological images were taken through the use of the Vanderbilt Cell Imaging Shared Resource. All the fixed tissue was processed by the Vanderbilt Translational Pathology Shared Resource. The author would like to thank Johannes Freudenberg and Lea Sarov-Blat for their assistance to locate microarray data.

Sources of Funding

This work was supported in part by NIH R01HL133290, R01HL119234, and R01HL143074 (to HL), R35HL144980 (to BCK), American Heart Association Atrial Fibrillation Strategically Focused Research Network Postdoctoral Fellowship 18SFRN34110369 (to KK).

Non-standard Abbreviations and Acronyms

AAV9	adeno-associated virus serotype 9
Ad-HIPK2	adenovirus expressing wild-type HIPK2 construct
Ad-HIPK2-KD	adenovirus expressing HIPK2 kinase-dead (K221A) construct
Ad-LacZ	adenovirus expressing LacZ construct
Ad-scrambled	adenovirus expressing shRNA-scrambled construct
Ad-shRNA-HIPK2	adenovirus expressing shRNA-HIPK2 construct
AKT	protein kinase B
αMHC	myosin heavy chain, α isoform
BAX	BCL2 associated X
BCL-XL	B-cell lymphoma-extra large
ChEA	ChIP enrichment analysis

CM	cardiomyocyte
COL1A1	collagen type I alpha 1 chain
COL1A2	collagen type I alpha 2 chain
EF	ejection fraction
EMMA	European Mouse Mutant Archive
ERK	extracellular signal-regulated kinase
FLP	B6.129S4-Gt(ROSA)26Sortm1(FLP1)Dym/RainJ24 mouse
FS	fractional shortening
GFP	green fluorescent protein
GSK3	glycogen synthase kinase 3
Het	heterozygous
HIPK2	homeodomain-interacting protein kinase 2
HIPK2^{tm2a}	C57BL/6NTac-Hipk2$^{tm2a(EUCOMM)Hmgu/Cnrm}$ mouse
HW/TL	heart weight normalized by tibia length
IPA	Ingenuity pathway analysis
JAK/STAT	the Janus kinase/signal transducers and activators of transcription
JNK	c-Jun N-terminal kinase
KO	knockout
LVID;d	left ventricle internal dimension at end-diastole
LVID;s	left ventricle internal dimension at end-systole
LVPW;d	left ventricle posterior wall thickness at end-diastole
LVPW;s	left ventricle posterior wall thickness at end-systole
MAPK	mitogen-activated protein kinase
MYH6	myosin heavy chain 6
MYH7	myosin heavy chain 7
NPPA	natriuretic peptide A
NPPB	natriuretic peptide B
NRF2	nuclear factor, erythroid 2 like 2

NRVM	neonatal rat ventricular cardiomyocyte
PI3K	phosphoinositide 3-kinase
PKC	protein kinase C
PWM	position weight matrix
qRT-PCR	real-time quantitative reverse transcription polymerase chain reaction
TAC	transaortic constriction
TF	transcription factor
TGFβ	transforming growth factor beta
TnT-MEK1-CA	troponin T-driven constitutively active mitogen-activated protein kinase kinase 1
TUNEL	terminal deoxynucleotidyl transferase dUTP nick end labeling
WT	wild-type
X2K	Expression2Kinases

Reference

1. Benjamin EJ, Muntner P, Alonso A, Bittencourt MS, Callaway CW, Carson AP, Chamberlain AM, Chang AR, Cheng S, Das SR, et al. Heart Disease and Stroke Statistics-2019 Update: A Report From the American Heart Association. Circulation. 2019;139(10):e56–e528. doi:10.1161/CIR.0000000000000659 [PubMed: 30700139]
2. Manning G, Whyte DB, Martinez R, Hunter T, Sudarsanam S. The protein kinase complement of the human genome. Science. 2002;298(5600):1912–1934. doi:10.1126/science.1075762 [PubMed: 12471243]
3. Caenepeel S, Charydczak G, Sudarsanam S, Hunter T, Manning G. The mouse kinome: Discovery and comparative genomics of all mouse protein kinases. Proc Natl Acad Sci. 2004;101(32):11707–11712. doi:10.1073/pnas.0306880101 [PubMed: 15289607]
4. Fuller SJ, Osborne SA, Leonard SJ, Hardyman MA, Vaniotis G, Allen BG, Sugden PH, Clerk A. Cardiac protein kinases: the cardiomyocyte kinome and differential kinase expression in human failing hearts. Cardiovasc Res. 2015;108(1):87–98. doi:10.1093/cvr/cvv210 [PubMed: 26260799]
5. Van Berlo JH, Maillet M, Molkentin JD. Signaling effectors underlying pathologic growth and remodeling of the heart. J Clin Invest. 2013;123(1):37–45. doi:10.1172/JCI62839 [PubMed: 23281408]
6. Vlahos CJ, McDowell SA, Clerk A. Kinases as therapeutic targets for heart failure. Nat Rev Drug Discov. 2003;2(2):99–113. doi:10.1038/nrd1009 [PubMed: 12563301]
7. Chen EY, Xu H, Gordonov S, Lim MP, Perkins MH, Ma'ayan A. Expression2Kinases: mRNA profiling linked to multiple upstream regulatory layers. Bioinformatics. 2012;28(1):105–111. doi:10.1093/bioinformatics/btr625 [PubMed: 22080467]
8. Jin Y, Ratnam K, Chuang PY, Fan Y, Zhong Y, Dai Y, Mazloom AR, Chen EY, D'Agati V, Xiong H, et al. A systems approach identifies HIPK2 as a key regulator of kidney fibrosis. Nat Med. 2012;18(4):580–588. doi:10.1038/nm.2685 [PubMed: 22406746]

9. Saul VV, De La Vega L, Milanovic M, Krüger M, Braun T, Fritz-Wolf K, Becker K, Schmitz ML. HIPK2 kinase activity depends on cis-autophosphorylation of its activation loop. J Mol Cell Biol. 2013;5(1):27–38. doi:10.1093/jmcb/mjs053 [PubMed: 23000554]
10. Kim YH, Choi CY, Lee SJ, Conti MA, Kim Y. Homeodomain-interacting protein kinases, a novel family of co-repressors for homeodomain transcription factors. J Biol Chem. 1998;273(40):25875–25879. doi:10.1074/jbc.273.40.25875 [PubMed: 9748262]
11. Zhang J, Pho V, Bonasera SJ, Holzmann J, Tang AT, Hellmuth J, Tang S, Janak PH, Tecott LH, Huang EJ. Essential function of HIPK2 in TGFβ-dependent survival of midbrain dopamine neurons. Nat Neurosci. 2007;10(1):77–86. doi:10.1038/nn1816 [PubMed: 17159989]
12. Lee W, Swarup S, Chen J, Ishitani T, Verheyen EM. Homeodomain-interacting protein kinases (Hipks) promote Wnt/Wg signaling through stabilization of β-catenin/Arm and stimulation of target gene expression. Development. 2009;136(2):241–251. doi:10.1242/dev.025460 [PubMed: 19088090]
13. D'Orazi G, Cecchinelli B, Bruno T, Manni I, Higashimoto Y, Saito S, Gostissa M, Coen S, Marchetti A, Del Sal G, et al. Homeodomain-interacting protein kinase-2 phosphorylates p53 at Ser 46 and mediates apoptosis. Nat Cell Biol. 2002;4(1):11–20. doi:10.1038/ncb714 [PubMed: 11780126]
14. Puca R, Nardinocchi L, Givol D, D'Orazi G. Regulation of p53 activity by HIPK2: Molecular mechanisms and therapeutical implications in human cancer cells. Oncogene. 2010;29(31):4378–4387. doi:10.1038/onc.2010.183 [PubMed: 20514025]
15. Torrente L, Sanchez C, Moreno R, Chowdhry S, Cabello P, Isono K, Koseki H, Honda T, Hayes JD, Dinkova-Kostova AT, et al. Crosstalk between NRF2 and HIPK2 shapes cytoprotective responses. Oncogene. 2017;36(44):6204–6212. doi:10.1038/onc.2017.221 [PubMed: 28692050]
16. Hofmann TG, Stollberg N, Schmitz ML, Will H. HIPK2 regulates transforming growth factor-beta-induced c-Jun NH(2)-terminal kinase activation and apoptosis in human hepatoma cells. Cancer Res. 2003;63(23):8271–8277. [PubMed: 14678985]
17. Lee S, Shang Y, Redmond SA, Urisman A, Tang AA, Li KH, Burlingame AL, Pak RA, Jovičić A, Gitler AD, et al. Activation of HIPK2 Promotes ER Stress-Mediated Neurodegeneration in Amyotrophic Lateral Sclerosis. Neuron. 2016;91(1):41–55. doi:10.1016/j.neuron.2016.05.021 [PubMed: 27321923]
18. Blaquiere JA, Verheyen EM. Homeodomain-Interacting Protein Kinases: Diverse and Complex Roles in Development and Disease. Curr Top Dev Biol. 2017;123:73–103. doi:10.1016/bs.ctdb.2016.10.002 [PubMed: 28236976]
19. Rinaldo C, Siepi F, Prodosmo A, Soddu S. HIPKs: Jack of all trades in basic nuclear activities. Biochim Biophys Acta - Mol Cell Res. 2008;1783(11):2124–2129. doi:10.1016/j.bbamcr.2008.06.006
20. Rinaldo C, Prodosmo A, Siepi F, Soddu S. HIPK2: a multitalented partner for transcription factors in DNA damage response and developmentThis paper is one of a selection of papers published in this Special Issue, entitled 28th International West Coast Chromatin and Chromosome Conference, and has. Biochem Cell Biol. 2007;85(4):411–418. doi:10.1139/o07-071 [PubMed: 17713576]
21. Liu X, Xiao J, Zhu H, Wei X, Platt C, Damilano F, Xiao C, Bezzerides V, Boström P, Che L, et al. MiR-222 is necessary for exercise-induced cardiac growth and protects against pathological cardiac remodeling. Cell Metab. 2015;21(4):584–595. doi:10.1016/j.cmet.2015.02.014 [PubMed: 25863248]
22. Wiggins AK, Wei G, Doxakis E, Wong C, Tang AA, Zang K, Luo EJ, Neve RL, Reichardt LF, Huang EJ. Interaction of Brn3a and HIPK2 mediates transcriptional repression of sensory neuron survival. J Cell Biol. 2004;167(2):257–267. doi:10.1083/jcb.200406131 [PubMed: 15492043]
23. Skarnes WC, Rosen B, West AP, Koutsourakis M, Bushell W, Iyer V, Mujica AO, Thomas M, Harrow J, Cox T, et al. A conditional knockout resource for the genome-wide study of mouse gene function. Nature. 2011;474(7351):337–342. doi:10.1038/nature10163 [PubMed: 21677750]
24. Henrich VC, Vogtli ME, Antoniewski C, Spindler-Barth M, Przibilla S, Noureddine M, Lezzi M. Widespread recombinase expression using FLPeR (flipper) mice. Genesis. 2000;28(3–4):106–110. doi:10.1002/1526-968X(200011/12)28:3/4<106::AID-GENE30>3.0.CO;2-T [PubMed: 11105051]

25. Agah R, Frenkel PA, French BA, Michael LH, Overbeek PA, Schneider MD. Gene recombination in postmitotic cells: Targeted expression of Cre recombinase provokes cardiac-restricted, site-specific rearrangement in adult ventricular muscle in vivo. J Clin Invest. 1997;100(1):169–179. doi:10.1172/JCI119509 [PubMed: 9202069]
26. Dufour BD, Smith CA, Clark RL, Walker TR, Mcbride JL. Intrajugular VEIN DELIVERY OF AAV9-RNAi prevents neuropathological changes and weight loss in huntington's disease mice. Mol Ther. 2014;22(4):797–810. doi:10.1038/mt.2013.289 [PubMed: 24390280]
27. Berger SI, Posner JM, Ma'ayan A. Genes2Networks: connecting lists of gene symbols using mammalian protein interactions databases. BMC Bioinformatics. 2007;8(1):372. doi:10.1186/1471-2105-8-372 [PubMed: 17916244]
28. Lachmann A, Ma'ayan A. KEA: Kinase enrichment analysis. Bioinformatics. 2009;25(5):684–686. doi:10.1093/bioinformatics/btp026 [PubMed: 19176546]
29. Sjolund J, Pelorosso FG, Quigley DA, DelRosario R, Balmain A. Identification of Hipk2 as an essential regulator of white fat development. Proc Natl Acad Sci U S A. 2014;111(20):7373–7378. doi:10.1073/pnas.1322275111 [PubMed: 24785298]
30. Chalazonitis A, Tang AA, Shang Y, Pham TD, Hsieh I, Setlik W, Gershon MD, Huang EJ. Homeodomain interacting protein kinase 2 regulates postnatal development of enteric dopaminergic neurons and glia via BMP signaling. J Neurosci. 2011;31(39):13746–13757. doi:10.1523/JNEUROSCI.1078-11.2011 [PubMed: 21957238]
31. Shang Y, Doan CN, Arnold TD, Lee S, Tang A a, Reichardt LF, Huang EJ. Transcriptional corepressors HIPK1 and HIPK2 control angiogenesis via TGF-β-TAK1-dependent mechanism. PLoS Biol. 2013;11(4):e1001527. doi:10.1371/journal.pbio.1001527 [PubMed: 23565059]
32. Hattangadi SM, Burke KA, Lodish HF. Homeodomain-interacting protein kinase 2 plays an important role in normal terminal erythroid differentiation. Blood. 2010;115(23):4853–4861. doi:10.1182/blood-2009-07-235093 [PubMed: 20231426]
33. Hwang HS, Kryshtal DO, Feaster TK, Sánchez-Freire V, Zhang J, Kamp TJ, Hong CC, Wu JC, Knollmann BC. Comparable calcium handling of human iPSC-derived cardiomyocytes generated by multiple laboratories. J Mol Cell Cardiol. 2015;85:79–88. doi:10.1016/J.YJMCC.2015.05.003 [PubMed: 25982839]
34. Saul VV, Schmitz ML. Posttranslational modifications regulate HIPK2, a driver of proliferative diseases. J Mol Med. 2013;91(9):1051–1058. doi:10.1007/s00109-013-1042-0 [PubMed: 23616089]
35. Kehat I, Davis J, Tiburcy M, Accornero F, Saba-El-Leil MK, Maillet M, York AJ, Lorenz JN, Zimmermann WH, Meloche S, et al. Extracellular signal-regulated kinases 1 and 2 regulate the balance between eccentric and concentric cardiac growth. Circ Res. 2011;108(2):176–183. doi:10.1161/CIRCRESAHA.110.231514 [PubMed: 21127295]
36. Kim YH, Choi CY, Lee SJ, Conti MA, Kim Y. Homeodomain-interacting protein kinases, a novel family of co-repressors for homeodomain transcription factors. J Biol Chem. 1998;273(40):25875–25879. doi:10.1074/jbc.273.40.25875 [PubMed: 9748262]
37. Möller A, Sirma H, Hofmann TG, Rueffer S, Klimczak E, Dröge W, Will H, Schmitz ML. PML is required for homeodomain-interacting protein kinase 2 (HIPK2)-mediated p53 phosphorylation and cell cycle arrest but is dispensable for the formation of HIPK domains. Cancer Res. 2003;63(15):4310–4314. http://www.ncbi.nlm.nih.gov/pubmed/12907596. Accessed February 8, 2018. [PubMed: 12907596]
38. Bueno OF, De Windt LJ, Tymitz KM, Witt S a, Kimball TR, Klevitsky R, Hewett TE, Jones SP, Lefer DJ, Peng CF, et al. The MEK1-ERK1/2 signaling pathway promotes compensated cardiac hypertrophy in transgenic mice. EMBO J. 2000;19(23):6341–6350. doi:10.1093/emboj/19.23.6341 [PubMed: 11101507]
39. Burchfield JS, Xie M, Hill J a. Pathological ventricular remodeling: mechanisms: part 1 of 2. Circulation. 2013;128(4):388–400. doi:10.1161/CIRCULATIONAHA.113.001878 [PubMed: 23877061]
40. Feng Y, Zhou L, Sun X, Li Q. Homeodomain-interacting protein kinase 2 (HIPK2): a promising target for anti-cancer therapies. Oncotarget. 2017;8(12):20452–20461. doi:10.18632/oncotarget.14723 [PubMed: 28107201]

41. Vande Woude G, Ahn N, Hermann A, Matten W, Mansour S, Fukasawa K, Candia J, Rong S. Transformation of mammalian cells by constitutively active MAP kinase kinase. Science (80-). 2006;265(5174):966–970. doi:10.1126/science.8052857

42. Doxakis E, Huang EJ, Davies AM. Homeodomain-interacting protein kinase-2 regulates apoptosis in developing sensory and sympathetic neurons. Curr Biol. 2004;14(19):1761–1765. doi:10.1016/j.cub.2004.09.050 [PubMed: 15458648]

43. Isono K, Nemoto K, Li Y, Takada Y, Suzuki R, Katsuki M, Nakagawara A, Koseki H. Overlapping Roles for Homeodomain-Interacting Protein Kinases Hipk1 and Hipk2 in the Mediation of Cell Growth in Response to Morphogenetic and Genotoxic Signals. Mol Cell Biol. 2006;26(7):2758–2771. doi:10.1128/MCB.26.7.2758-2771.2006 [PubMed: 16537918]

44. Banks M, Crowell K, Proctor A, Jensen BC. Cardiovascular Effects of the MEK Inhibitor, Trametinib: A Case Report, Literature Review, and Consideration of Mechanism. Cardiovasc Toxicol. 2017;17(4):487–493. doi:10.1007/s12012-017-9425-z [PubMed: 28861837]

45. Yndestad A, Damås JK, Eiken HG, Holm T, Haug T, Simonsen S, Frøland SS, Gullestad L, Aukrust P. Enhanced myocyte contractility and Ca2+ handling in a calcineurin transgenic model of heart failure. Cardiovasc Res. 2002;54(1):105–116. doi:10.1016/S0008-6363(02)00230-4 [PubMed: 12062367]

46. Galindo CL, Singh AP, Lal H, Verma VK, Zhang Q, Force T, McNamara JW, Umbarkar P, Gupte M, Guo Y. Cardiomyocyte SMAD4-Dependent TGF-β Signaling is Essential to Maintain Adult Heart Homeostasis. JACC Basic to Transl Sci. 1 2019:265. doi:10.1016/j.jacbts.2018.10.003

47. Nugent MM, Lee K, He JC. HIPK2 is a new drug target for anti-fibrosis therapy in kidney disease. Front Physiol. 2015;6(4):132. doi:10.3389/fphys.2015.00132 [PubMed: 25972814]

Clinical Perspective

What is new?

- We report a novel cardiac kinase HIPK2 as a potential regulator in heart failure.
- Cardiac HIPK2 expression is elevated in adult compared to the embryonal and neonatal stage, but down-regulated in failing hearts.
- Deletion of HIPK2 in cardiomyocytes leads to decreased heart function in adulthood.
- The cardiac effect of HIPK2 is correlated to its gene expression level.
- We discovered impaired ERK signaling as a main driver of HIPK2-deficient phenotype by enhancing apoptosis.
- AAV9 expressing constitutively active MEK1 largely rescued cardiac dysfunction in HIPK2 deficient hearts via restoration of ERK signaling.

What are the clinical implications?

- Since HIPK2 is protective in cardiomyocytes, gene therapy using HIPK2 could be a potential therapeutic method of heart failure treatment.
- As inhibition of HIPK2 has been proposed as a therapeutic approach for certain cancers and renal fibrosis, our study provides a caution for the potential cardiotoxicity of HIPK2 inhibition in the adult heart.

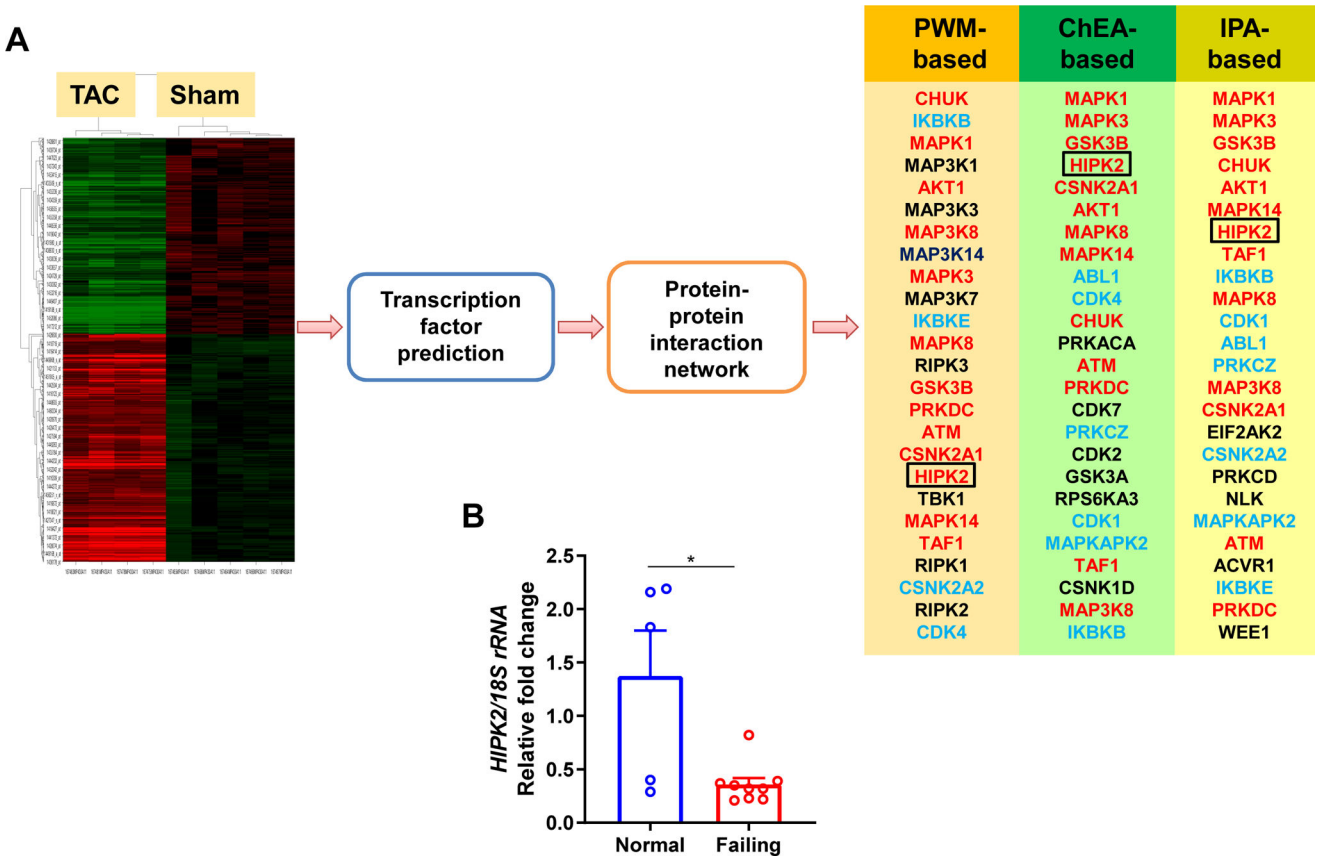

Figure 1. Identification of HIPK2 as a potential regulator of heart failure.

A. Adult C57BJ6 male mice were subjected to transaortic constriction (TAC) or sham surgery. RNA samples from the 6-week post-TAC or sham mice were subjected to microarray analysis. Transcriptomic analysis was performed to identify differentially expressed genes between TAC versus sham group. Hierarchical clustering by these differentially expressed genes was performed with results as depicted in the heat map (green color denotes down-regulated genes; red color denotes up-regulated genes). Transcription factors (TF) were predicted based on these gene expression changes by using three approaches based on Ingenuity Pathway Analysis (IPA), Position Weight Matrix (PWM), and ChIP Enrichment Analysis (ChEA) algorithms, and then upstream kinases of those transcription factors were identified using Kinase Enrichment Analysis. Top kinase targets are represented in 3 columns for respective TF prediction methods used. Red: kinases identified by all 3 approaches; Blue: kinases identified by 2 approaches; Black: kinase identified by one approach. **B**. Quantification of HIPK2 mRNA expression in human normal hearts versus failing hearts. Normal hearts: n=5, failing hearts: n=9. * $p<0.05$, Mann-Whitney test. All bar graphs are represented by mean ± SEM.

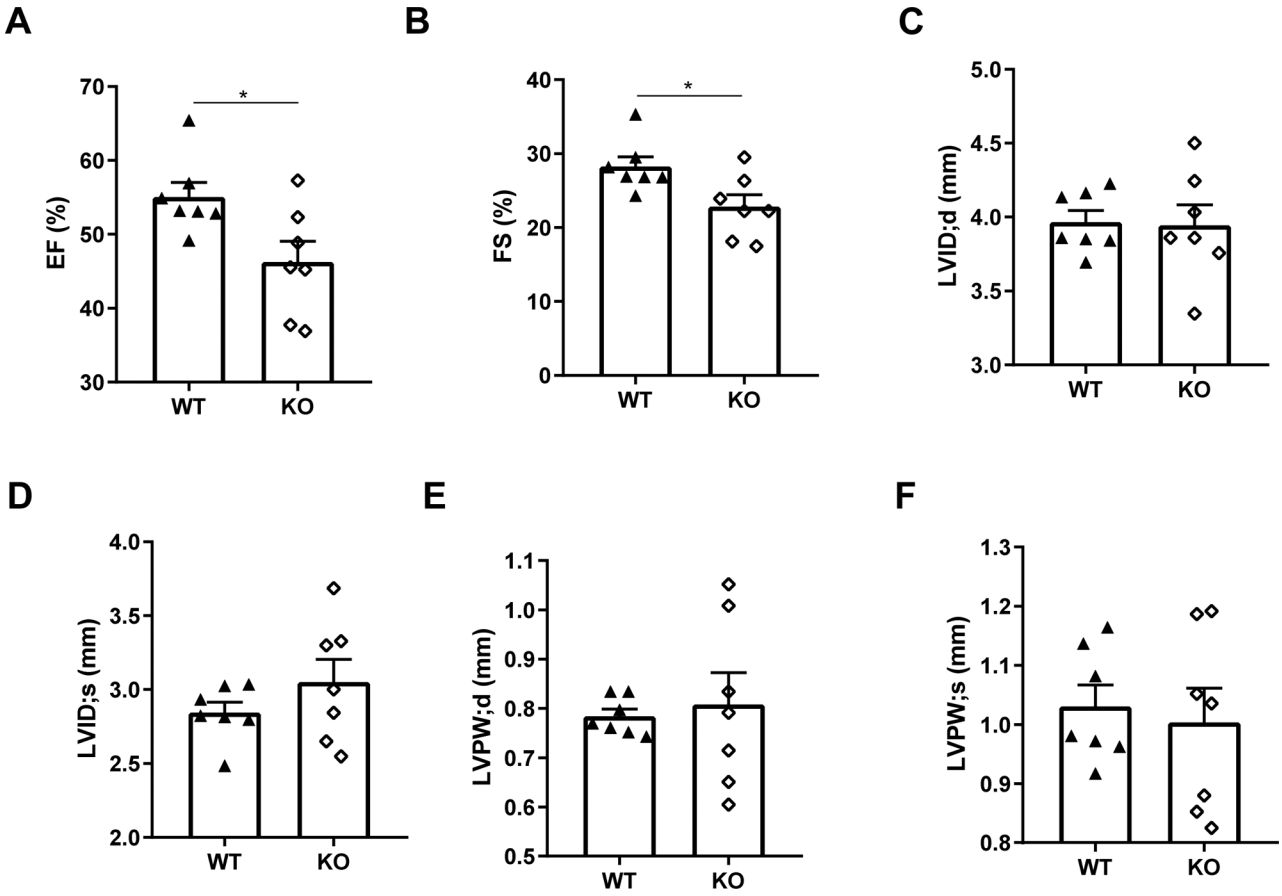

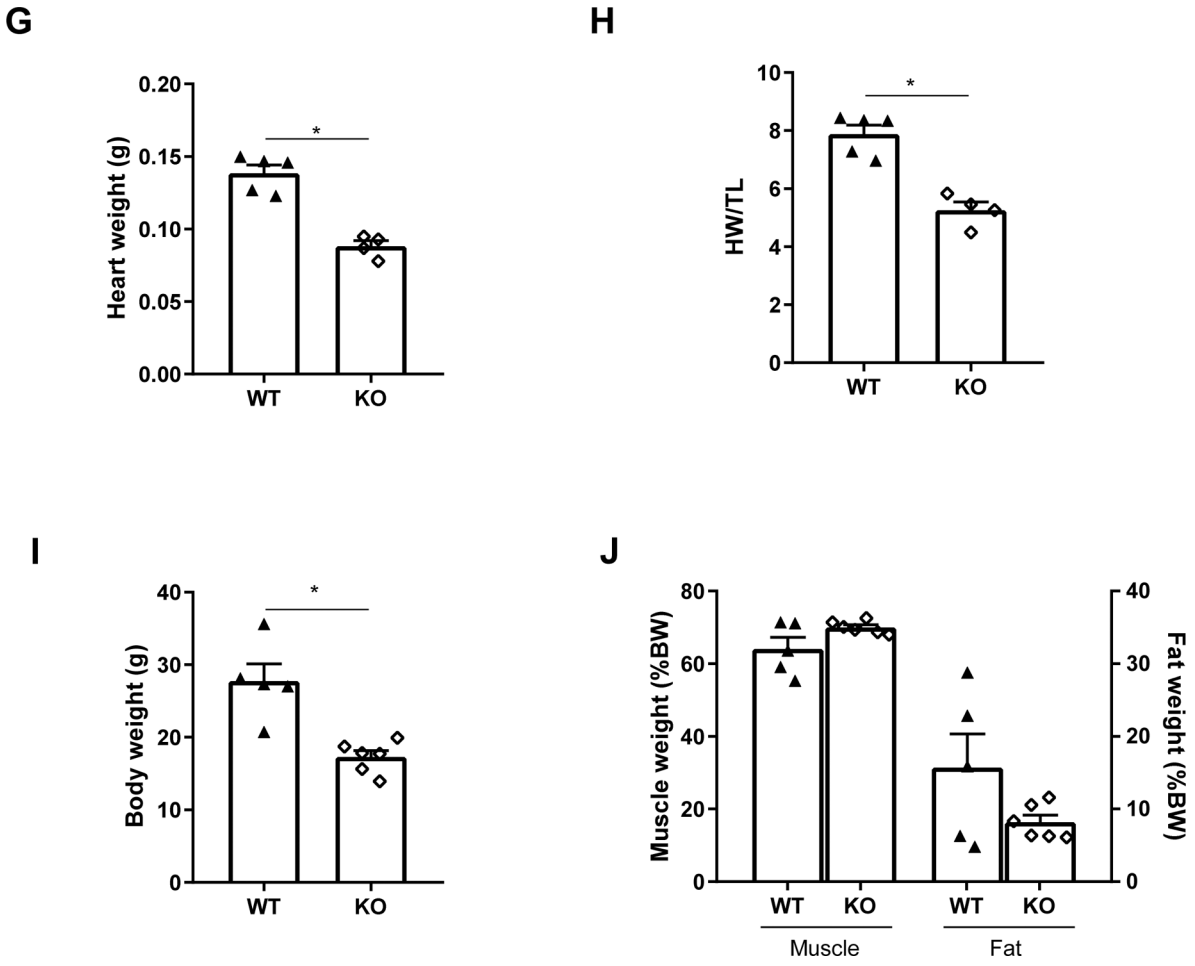

Figure 2. Phenotyping of HIPK2 global KO mice.

5-month-old KO and WT mice were examined by transthoracic echocardiogram. **A**. Ejection fraction (EF). **B**. Fractional shortening (FS). **C**. Left ventricle internal dimension at end-diastole (LVID; d). **D**. Left ventricle internal dimension at end-systole (LVID; s). **E**. Left ventricle posterior wall thickness at end-diastole (LVPW; d). **F**. Left ventricle posterior wall thickness at end-systole (LVPW; s). **G**. Heart weight. **H**. Heart weight normalized by tibia length (HW/TL). **I**. Body weight. **J**. Body composition: muscle weight and fat weight was measured by Nuclear Magnetic Resonance analyzer. The percentage of muscle weight and fat weight was then calculated by dividing the muscle or fat weight by body weight. n=4–7 per group. * $p<0.05$, Mann-Whitney test.

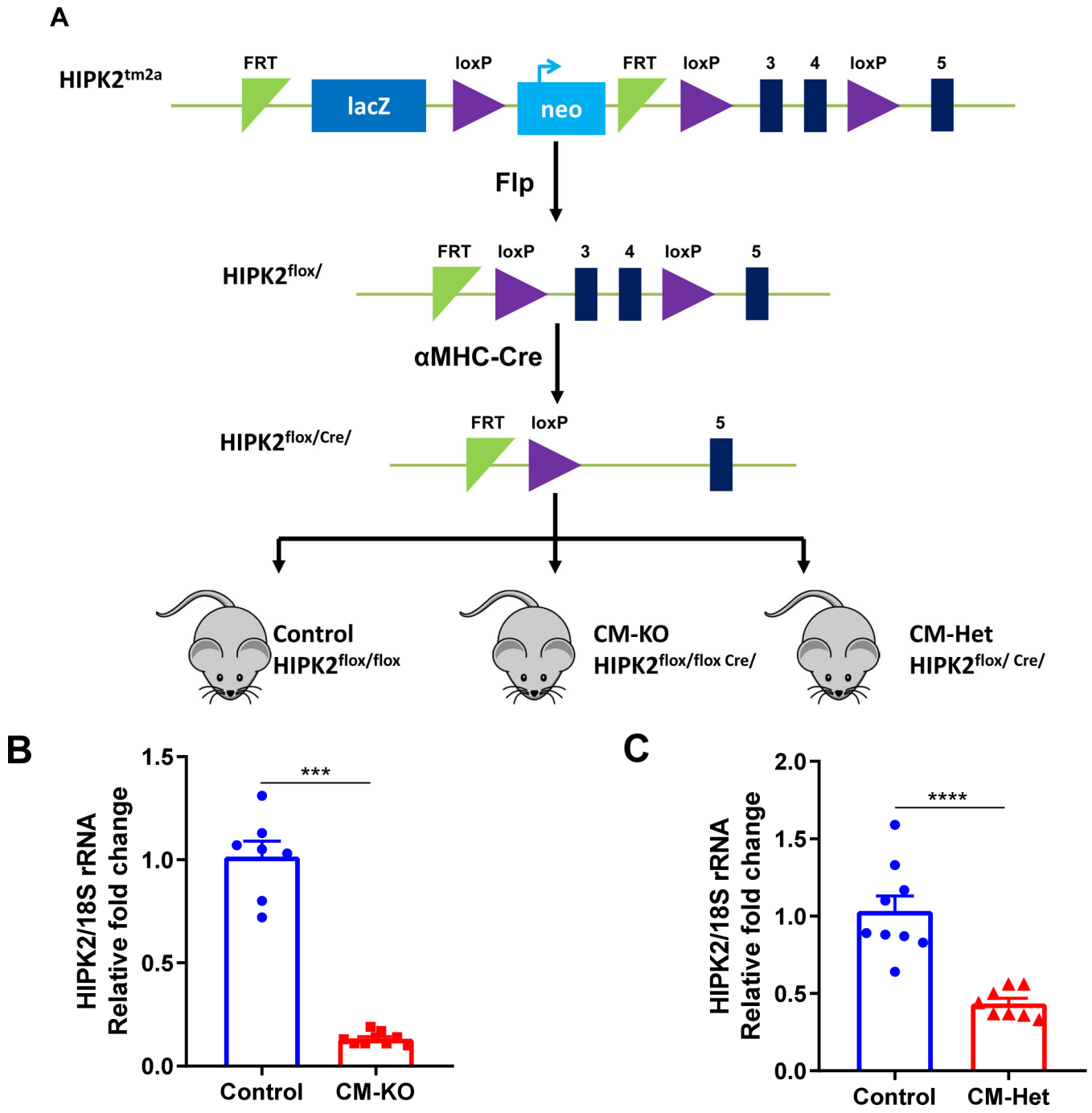

Figure 3. Generation of cardiomyocyte-specific HIPK2 KO mice.

A. Scheme of CM-specific HIPK2 KO and Het mice generation. HIPK2^{tm2a} mice from the European Mouse Mutant Archive (EMMA) were crossed with FLP mice to obtain mice with *HIPK2 flox* allele. Then, HIPK2$^{flox/flox}$ mice were crossed with αMHC-Cre mice to achieve CM-specific HIPK2 KO (HIPK2$^{flox/flox\ Cre/}$, CM-KO) or CM-specific HIPK2 Het (HIPK2$^{flox/Cre/}$, CM-Het) or littermate controls (HIPK2$^{flox/flox}$, Control). CM, cardiomyocyte. **B**. Quantification of *HIPK2* mRNA expression in the Control and CM-KO mouse left ventricle. n=7–9 per group. **C**. Quantification of HIPK2 mRNA expression in the

Control and CM-Het mouse left ventricle. n=8–9 per group. *** $p<0.005$, **** $p<0.0001$, Mann-Whitney test.

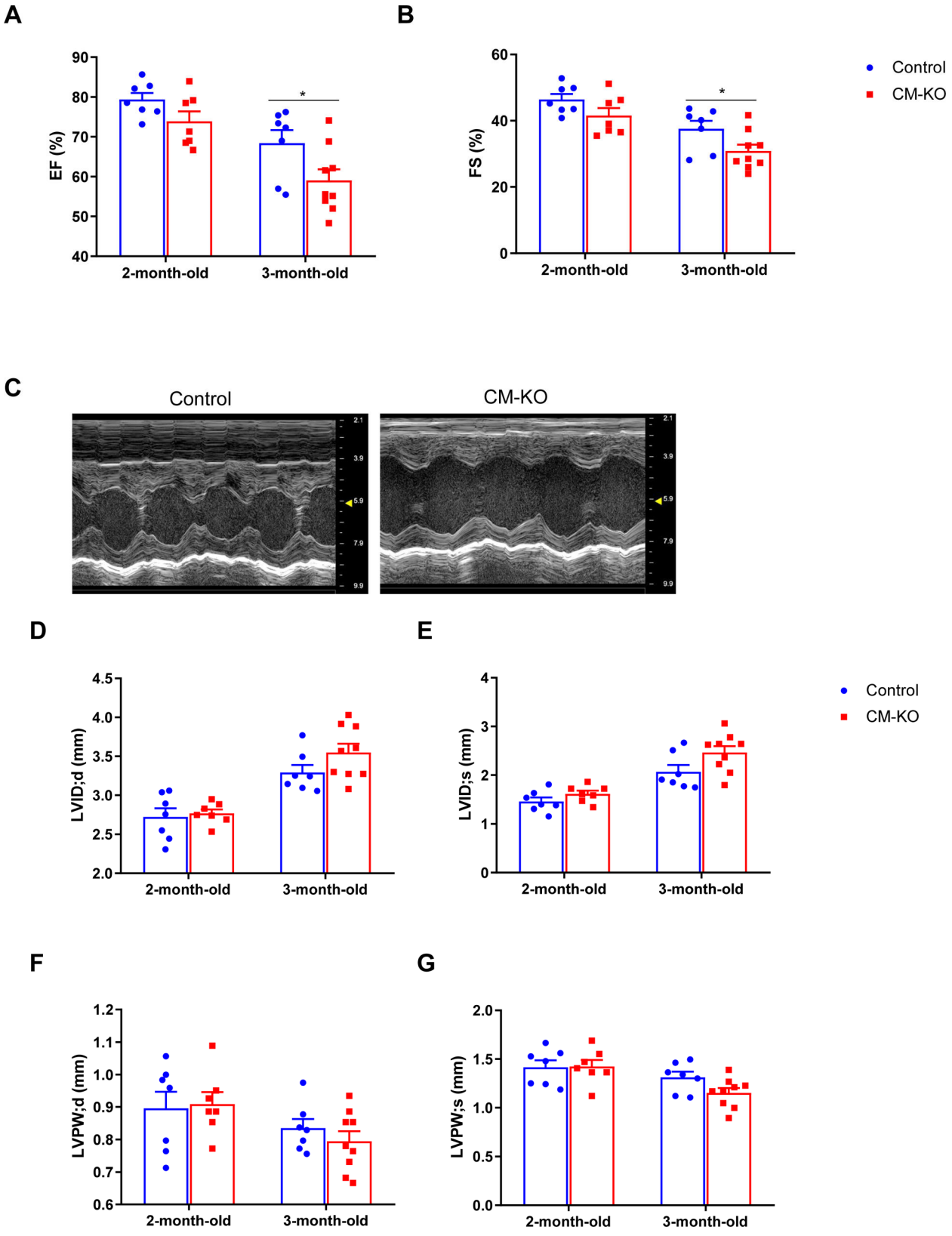

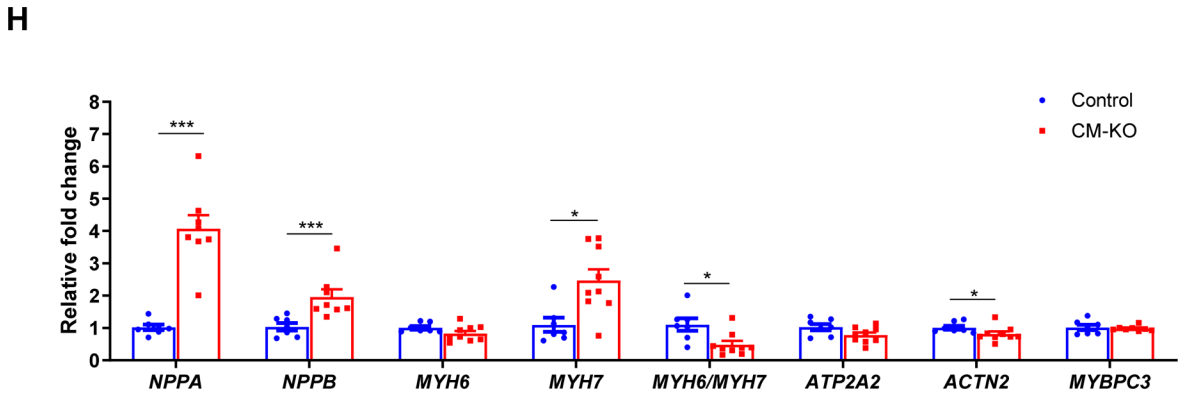

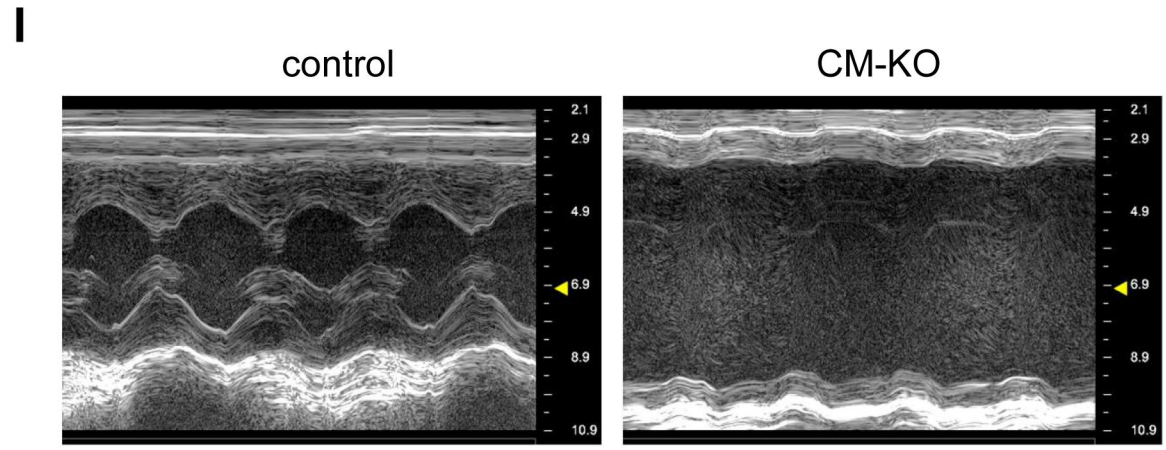

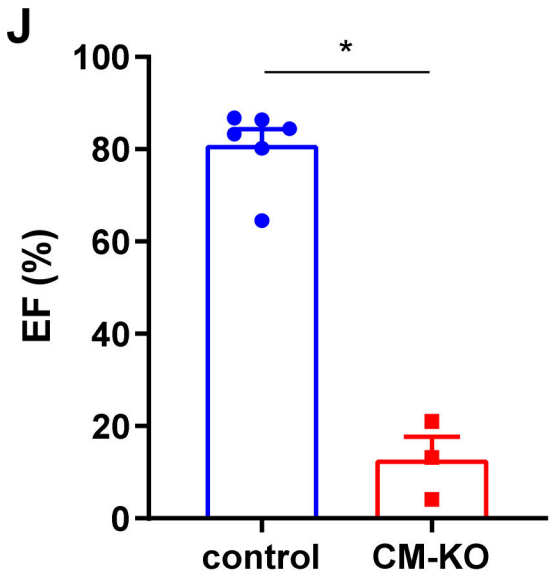

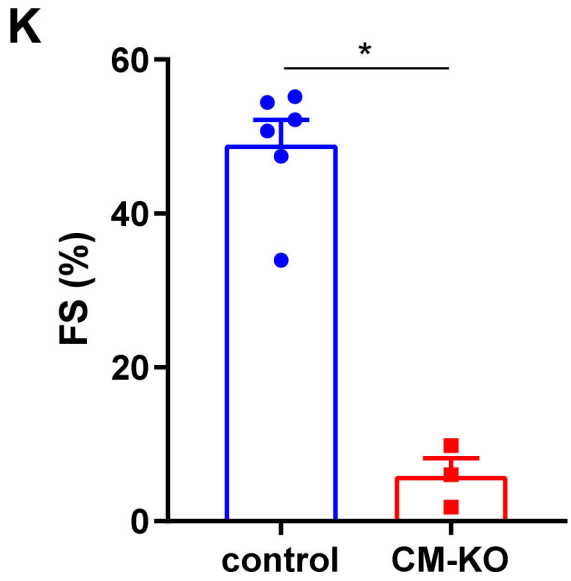

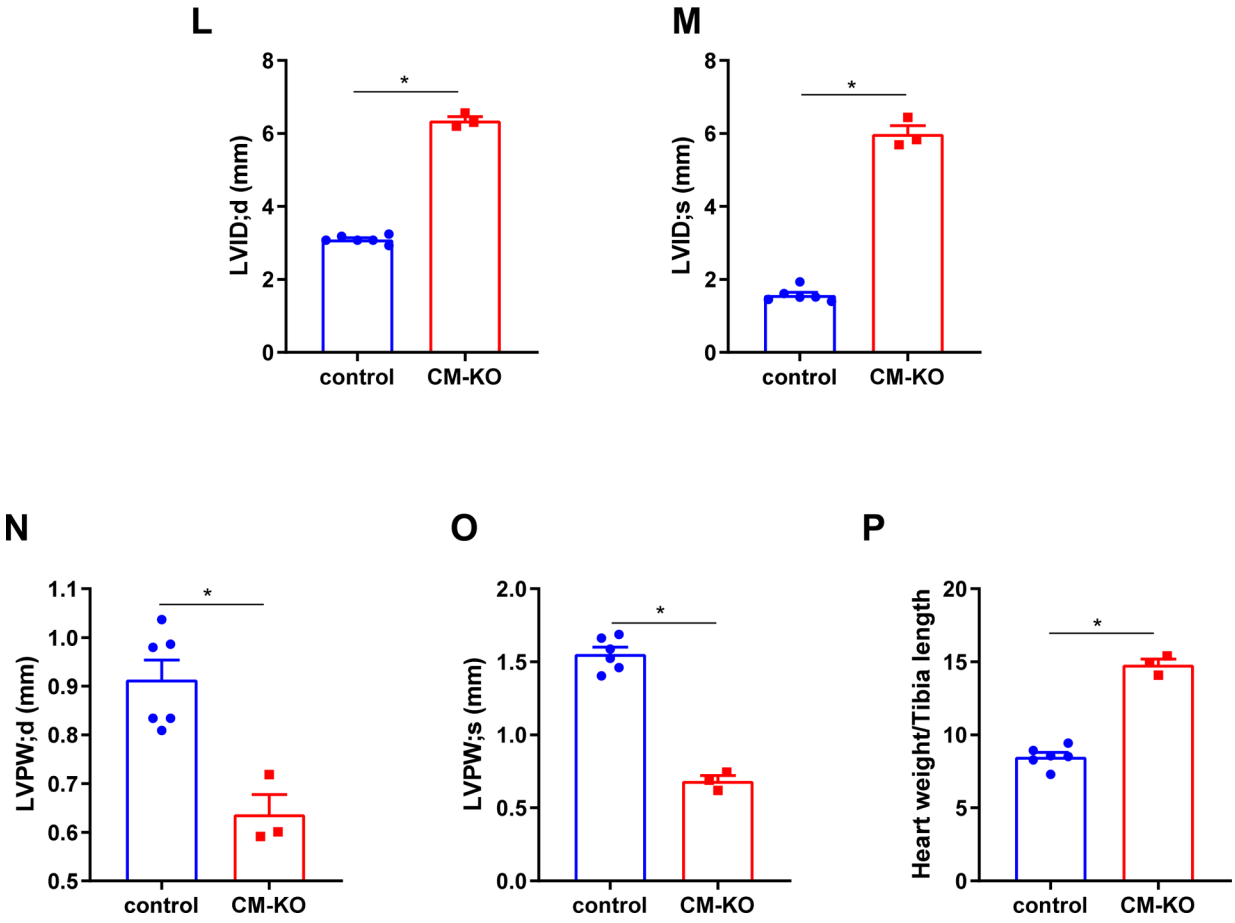

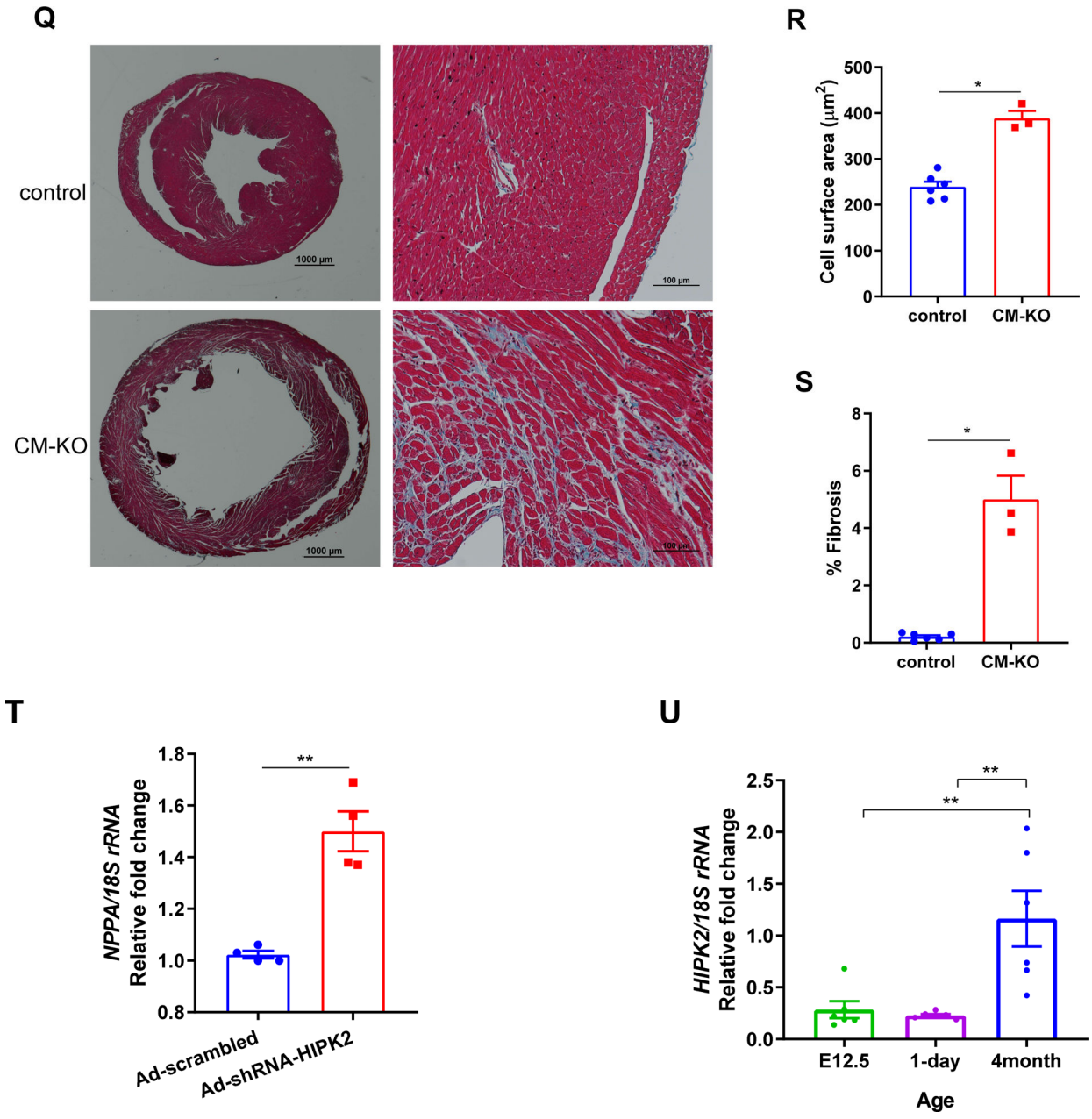

Figure 4. Cardiac function of CM-KO mice.

A-G: Heart function of CM-KO and littermate controls was measured by transthoracic echocardiogram at 2 months and 3 months of age. **A**. Ejection fraction. **B**. Fractional shortening.

C. Representative M-mode echocardiographic images of 3-month-old CM-KOs and Controls. **D**. Left ventricle internal dimension at end-diastole (LVID; d). **E**. Left ventricle internal dimension at end-systole (LVID; s). **F**. Left ventricle posterior wall thickness at end-diastole (LVPW; d). **G**. Left ventricle posterior wall thickness at end-systole (LVPW; s). n=7–9 per group. **H**. Quantification of mRNA expression of heart failure markers and sarcomere genes in 3-month-old CM-KO and Control LV. * $p<0.05$, *** $p<0.005$, Mann-

Whitney test. **I-O**: 8-month-old male CM-KO and control mice were examined by transthoracic echocardiogram. **I**. Representative M-mode echocardiographic images of 8-month-old CM-KOs and Controls. **J**. Ejection fraction (EF). **K**. Fractional shortening (FS). **L**. Left ventricle internal dimension at end-diastole (LVID; d). **M**. Left ventricle internal dimension at end-systole (LVID; s). **N**. Left ventricle posterior wall thickness at end-diastole (LVPW; d). **O**. Left ventricle posterior wall thickness at end-systole (LVPW; s). **P**. Heart weight normalized by tibia length (HW/TL). The control group contained 2 age-matched $HIPK2^{flox/flox}$ mice and 4 C57BJ6 mice. * $p<0.05$, Mann-Whitney test. **Q**. Representative images of Masson's Trichrome stained heart sections. **R**. Quantification of CM cross-sectional area. **S**. Quantification of fibrosis deposition. * $p<0.05$, Mann-Whitney test. **T**. NRVMs were infected with adenovirus expressing scrambled shRNA (Ad-scrambled) or shRNA-HIPK2 (Ad-shRNA-HIPK2) for 48 hours. qRT-PCR was performed to examine the mRNA expression of *NPPA*. n=4 independent replicates. ** $p<0.01$, unpaired t-test. **U**. Quantification of mRNA expression of *HIPK2* in the heart from E12.5, day 1, 4-month-old C57BL/6J mice. n=6 per group. **$p<0.01$, one-way ANOVA with Turkey's post hoc test.

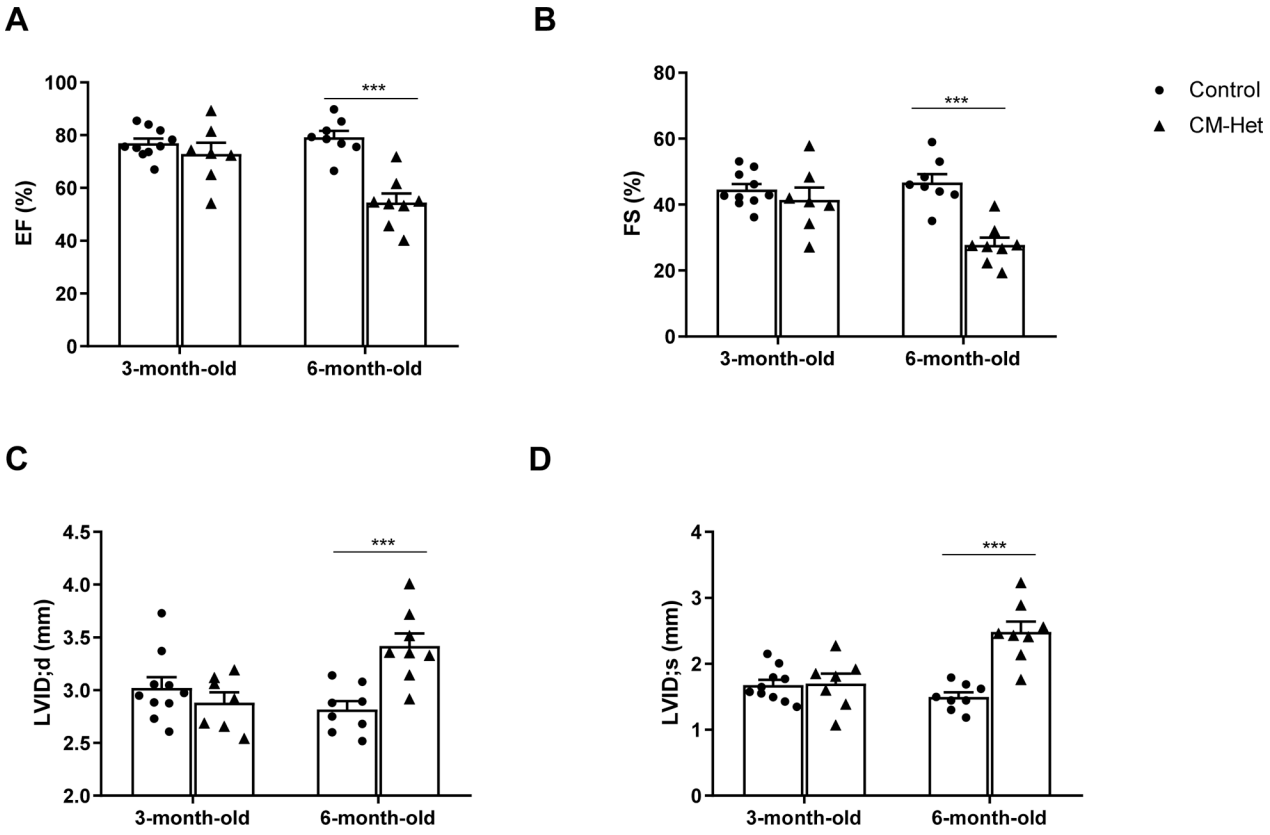

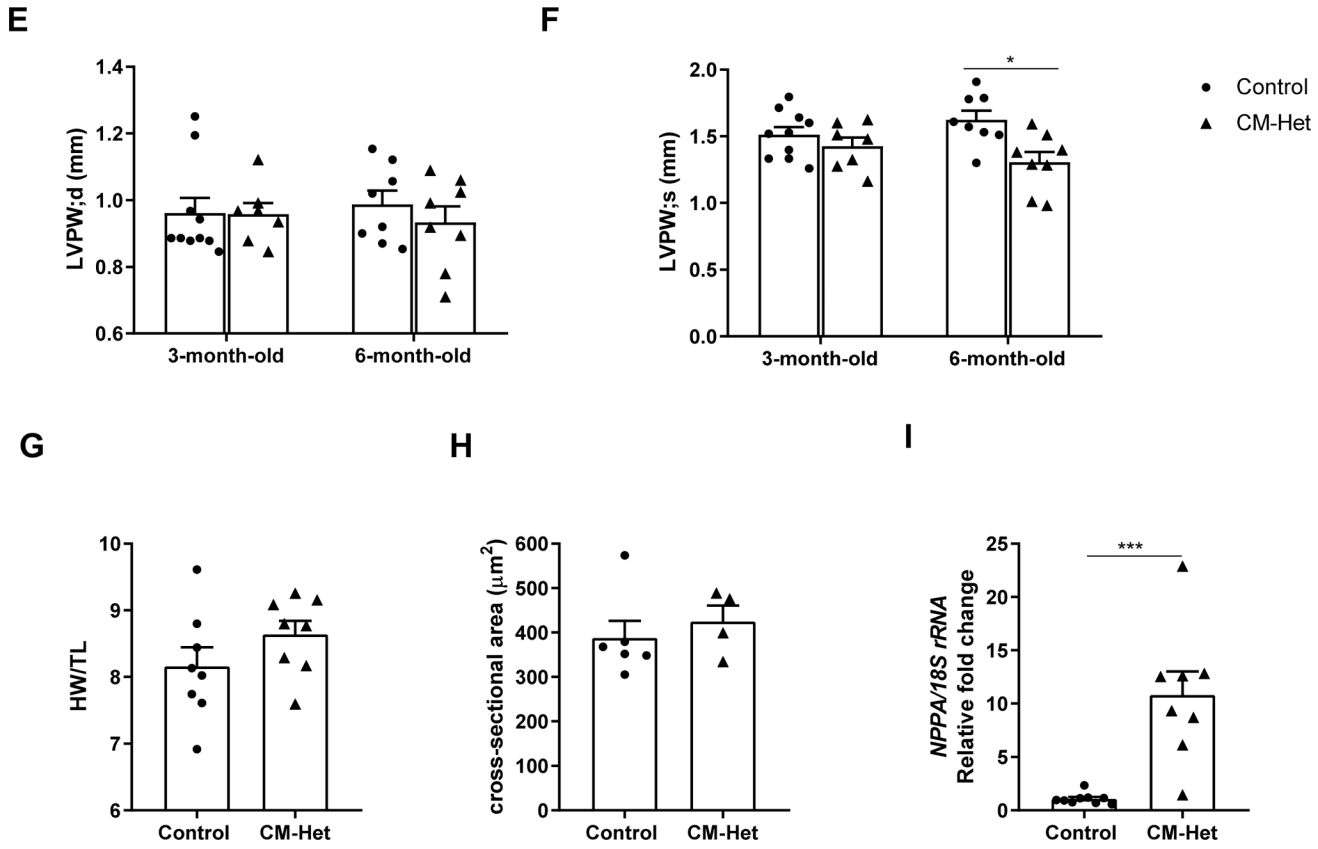

Figure 5. Cardiac function of CM-Het mice.

Heart function of CM-Het and Controls was measured by transthoracic echocardiogram at 3 months and 6 months of age. **A**. Ejection fraction. **B**. Fractional shortening. **C**. Left ventricle internal dimension at end-diastole (LVID; d). **D**. Left ventricle internal dimension at end-systole (LVID; s). **E**. Left ventricle posterior wall thickness at end-diastole (LVPW; d). **F**. Left ventricle posterior wall thickness at end-systole (LVPW; s). **G**. Heart weight normalized by tibia length. **H**. Quantification of CM cross-sectional area. **I**. Quantification of *NPPA* gene expression in CM-Het and Control left ventricle. n=7–10 per group. * $p<0.05$, *** $p<0.005$, Mann-Whitney test.

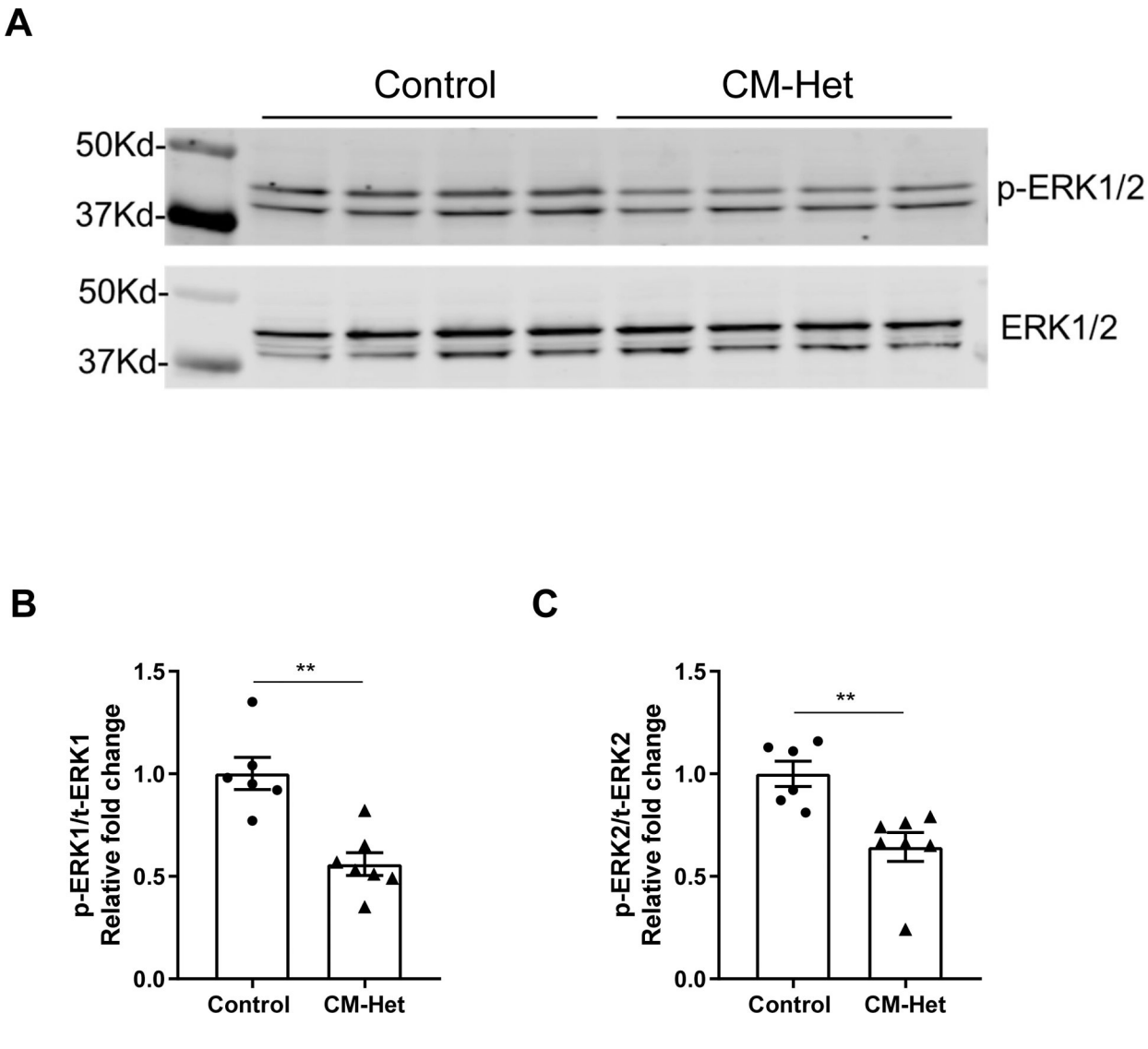

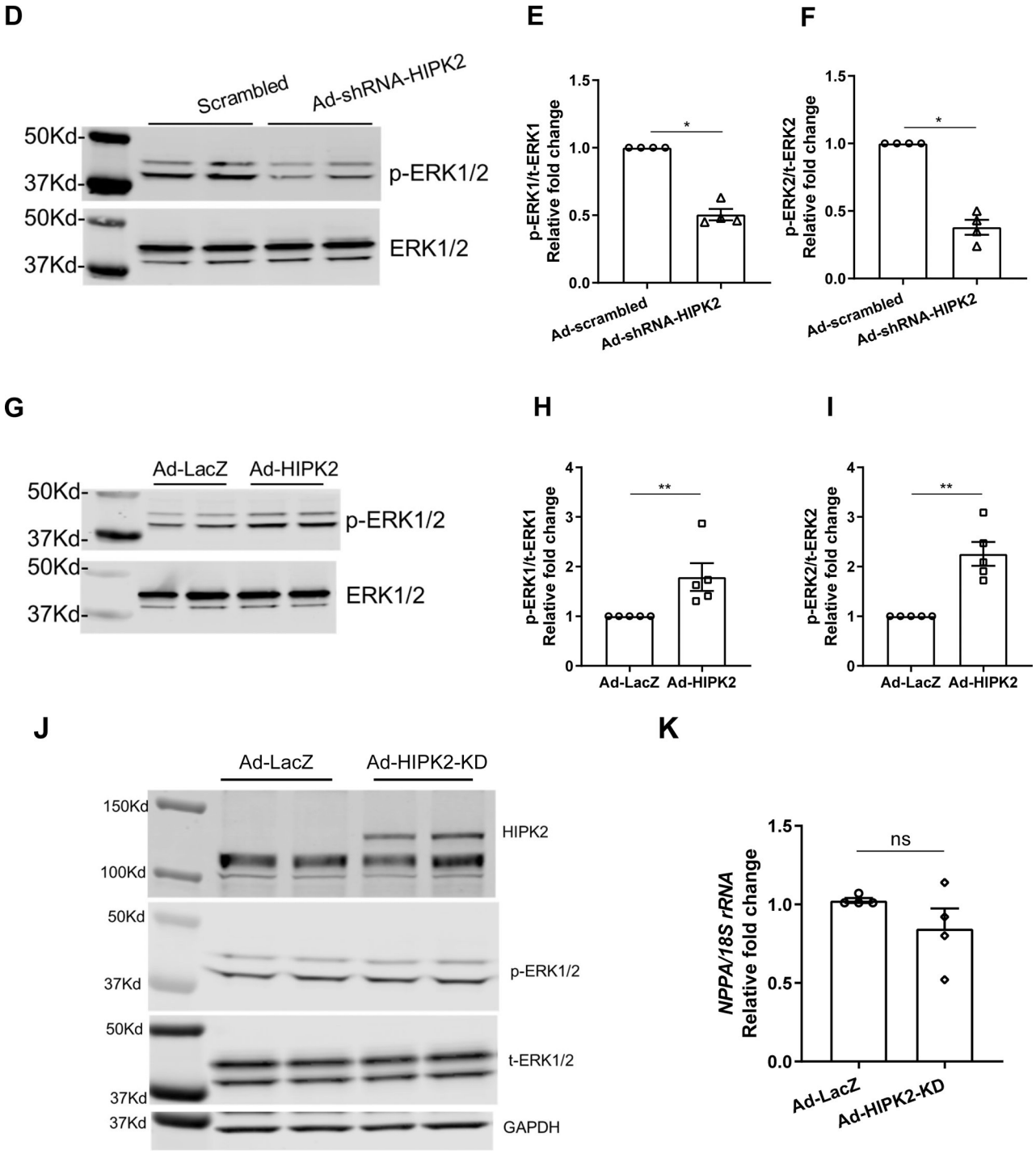

Figure 6. HIPK2 regulates ERK1/2 phosphorylation in the heart. A. Representative immunoblot showing significantly decreased ERK1 and ERK2 phosphorylation in the left ventricle of CM-Hets versus littermate Controls. **B-C.** Quantification of ERK1 and ERK2 phosphorylation in the left ventricle of CM-Het versus Controls. n=6–7 per group. * $p<0.05$, ** $p<0.01$, Mann-Whitney test. **D-K.** NRVMs were infected with adenovirus expressing scrambled shRNA (Scrambled), HIPK2 shRNA (Ad-

shRNA-HIPK2), LacZ (Ad-LacZ), HIPK2 (Ad-HIPK2), or HIPK2 kinase-dead (Ad-HIPK2-KD) virus. Western blot analysis was performed to determine the phosphorylation of ERK1 and ERK2. **D**. Representative immunoblot showing significantly decreased phosphorylation of ERK1 and ERK2 in HIPK2 knockdown group. **E-F**. Quantification of ERK1 and ERK2 phosphorylation in Ad-shRNA-HIPK2 group versus scrambled group. n=5 independent replicates. **G**. Representative immunoblot showing significantly increased phosphorylation of ERK1 and ERK2 in HIPK2 overexpression group. **H-I**. Quantification of ERK1 and ERK2 phosphorylation in Ad-HIPK2 group versus Ad-LacZ group. n=4 independent replicates. **J**. Representative immunoblot showing no change of phosphorylation of ERK1 and ERK2 in kinase-dead group. **K**. Quantification of mRNA expression of *NPPA* in NRVMs overexpressed with Ad-HIPK2-KD or Ad-LacZ. n=4 independent replicates. * $p<0.05$, ** $p<0.01$, Mann-Whitney test.

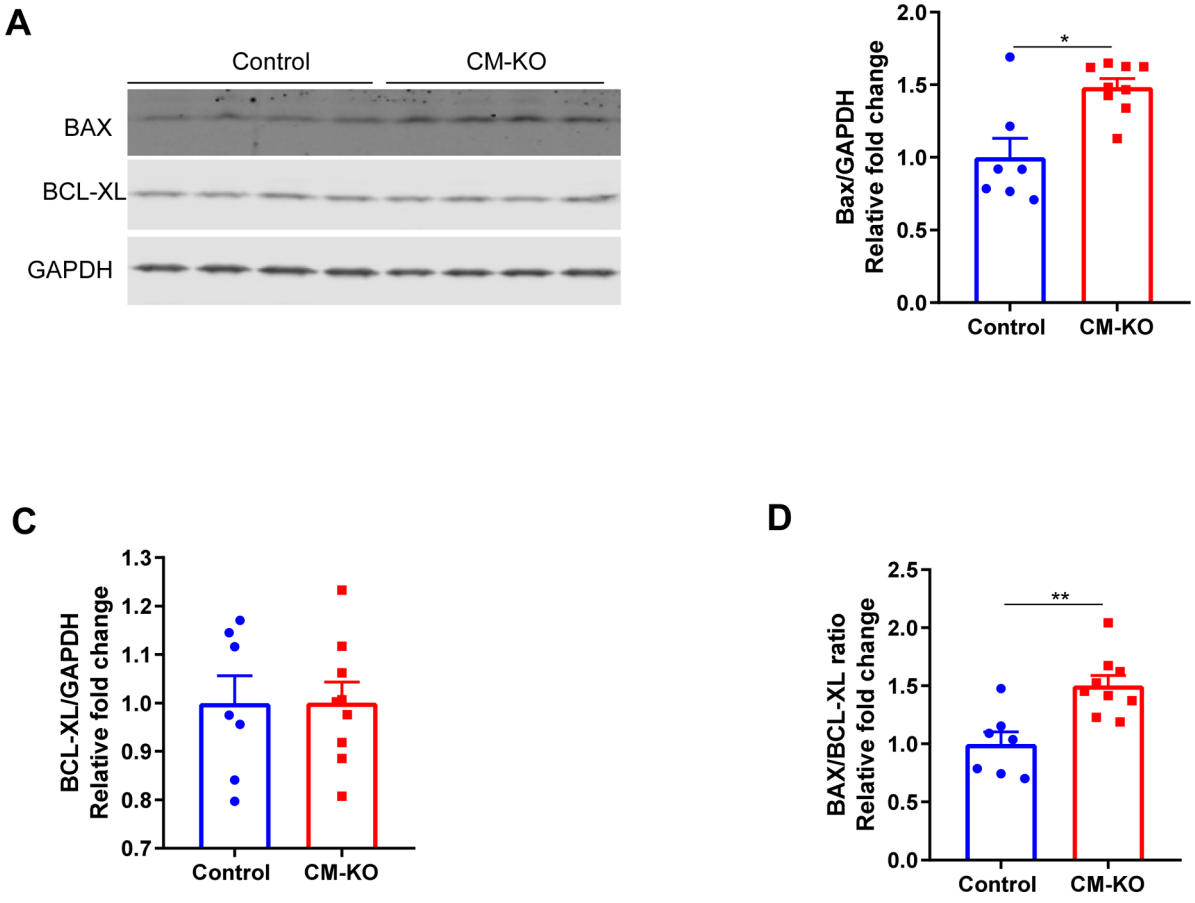

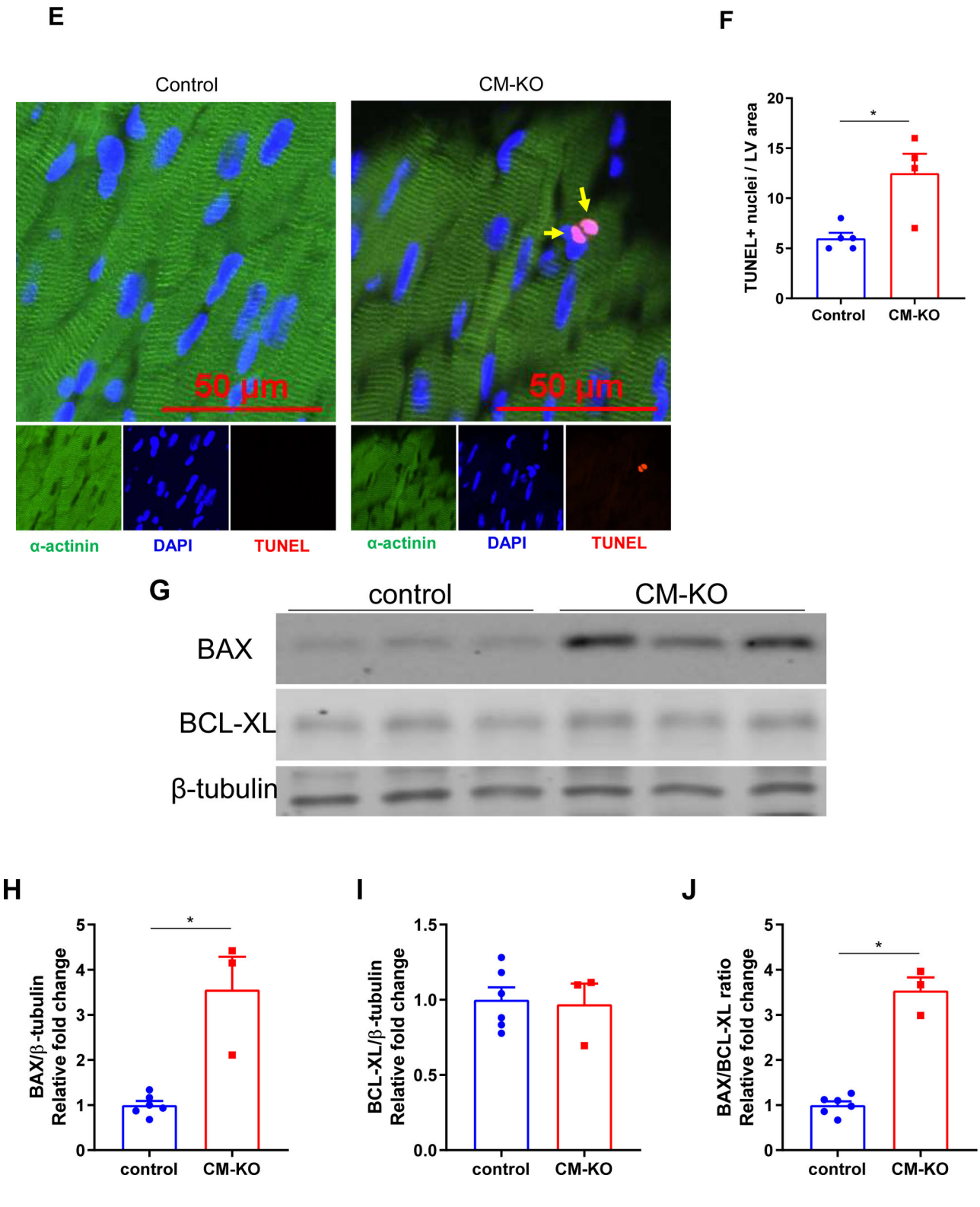

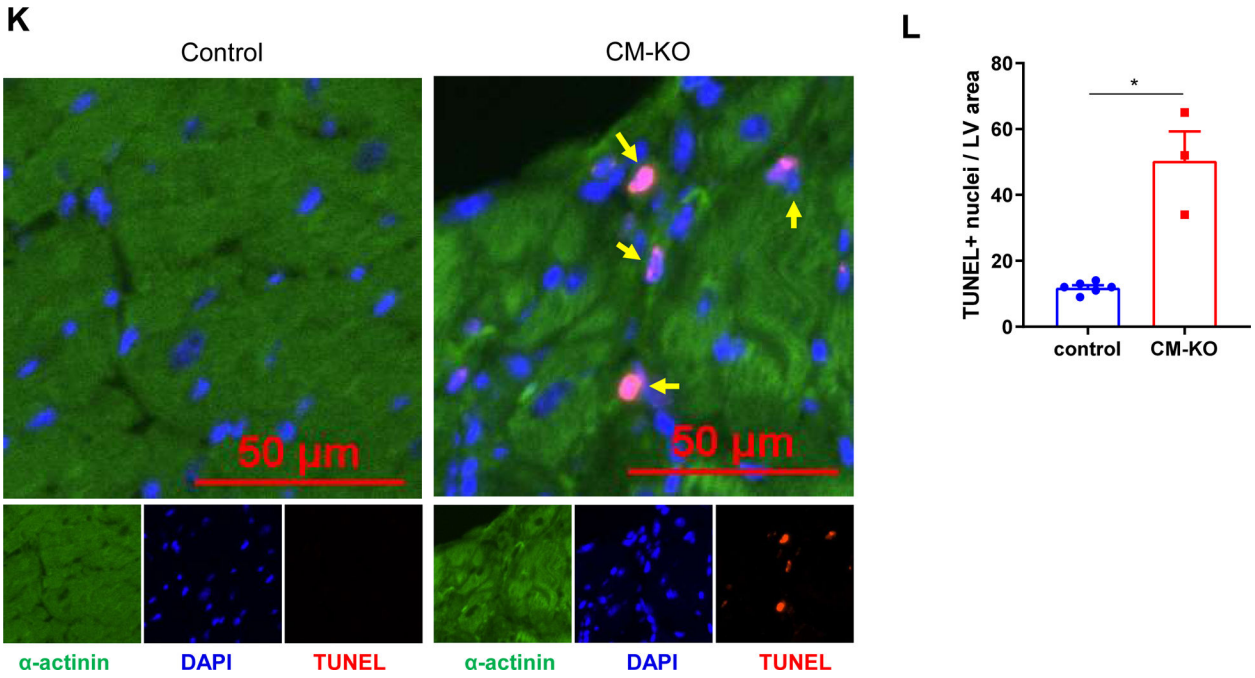

Figure 7. Enhanced apoptosis in CM-KO hearts. A-D.

Protein expression of regulators of apoptotic pathway were measured with Western blot in 3-month-old CM-KO and Control mice. **A**. Representative immunoblot showing expression of BCL-XL and BAX. **B-D**. Quantification of BAX, BCL-XL expression, and BAX/BCL-XL ratio in the 3-month-old CM-KO and Control LV. Control: n=7, CM-KO: n=9. **E**. Representative images of TUNEL positive CMs nuclei in the 3-month-old CM-KO and Control LV section. **F**. Quantification of TUNEL positive CM nuclei in the CM-KO and Control LV section. Control: n=5, CM-KO: n=4. * $p<0.05$, ** $p<0.01$, Mann-Whitney test. **G-L**. Protein expression of regulators of apoptotic pathway were measured with Western blot in 8-month-old CM-KO and control mice. **G**. Representative immunoblot showing expression of BCL-XL and BAX. **H-J**. Quantification of BAX, BCL-XL expression, and BAX/BCL-XL ratio in the 8-month-old CM-KO and Control LV. **K**. Representative images of TUNEL positive CMs nuclei in the CM-KO and Control LV section. **L**. Quantification of TUNEL positive CM nuclei in the CM-KO and Control LV section. control: n=6, CM-KO: n=3. The control group contained age-matched 2 $HIPK2^{flox/flox}$ mice and 4 C57BJ6. * $p<0.05$, Mann-Whitney test.

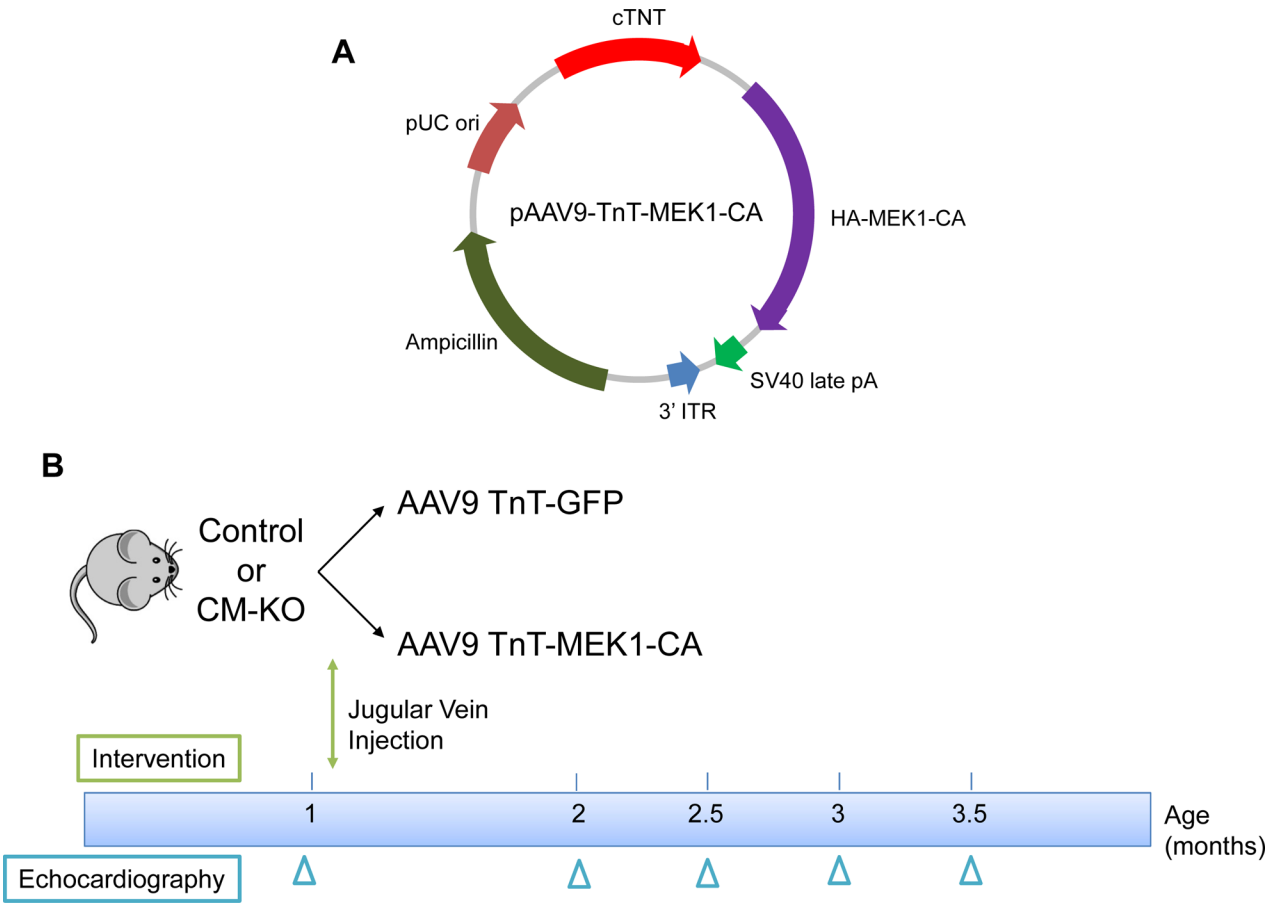

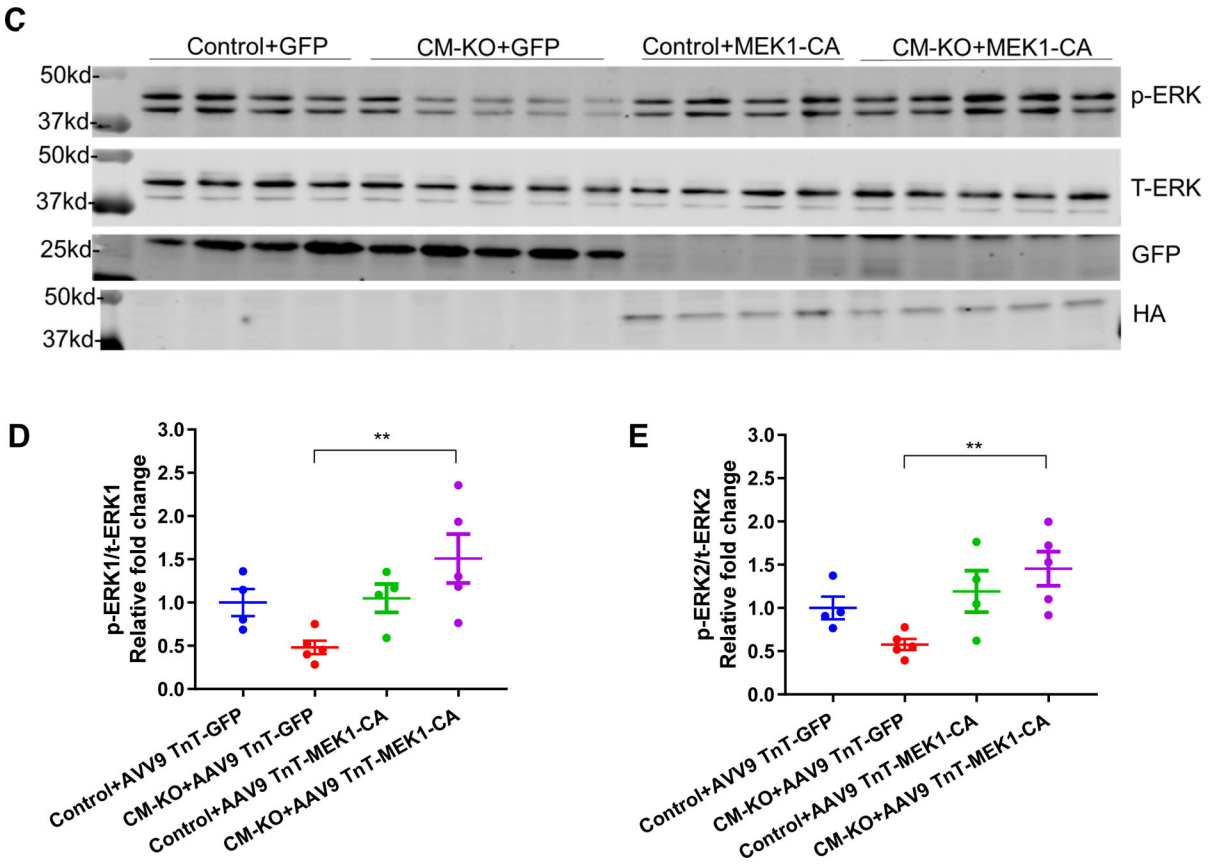

F

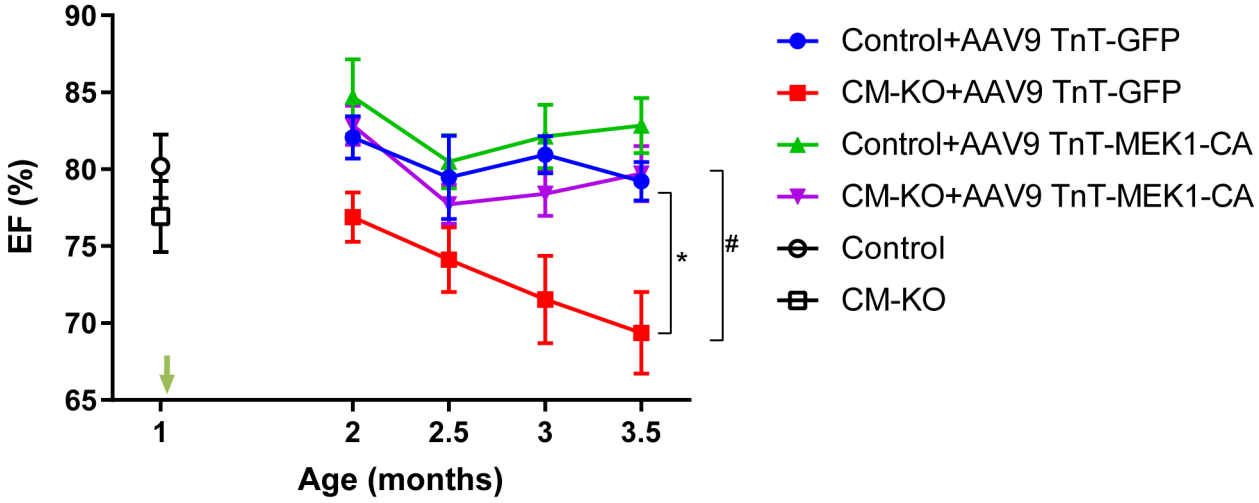

G

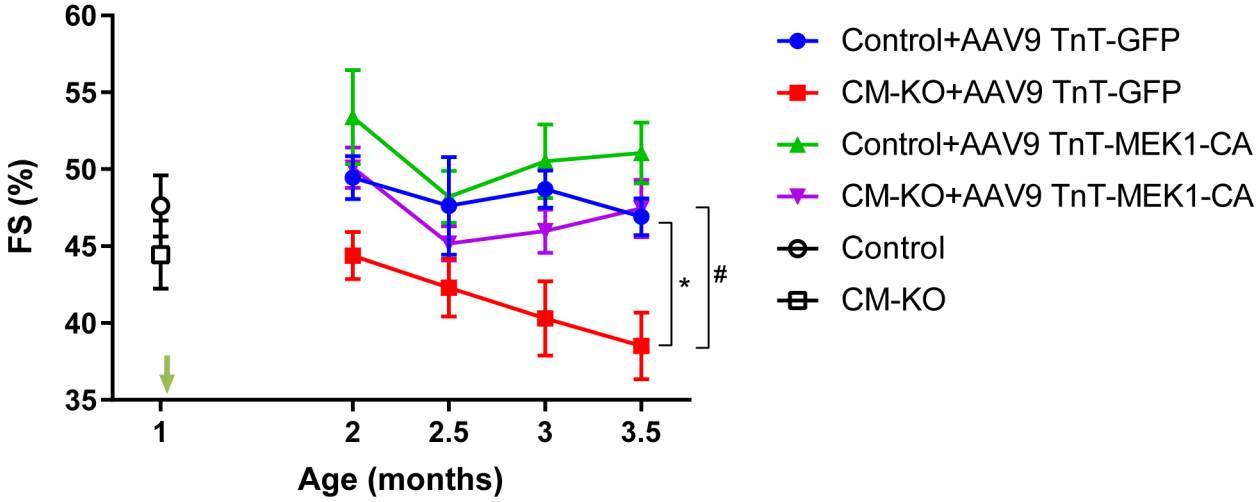

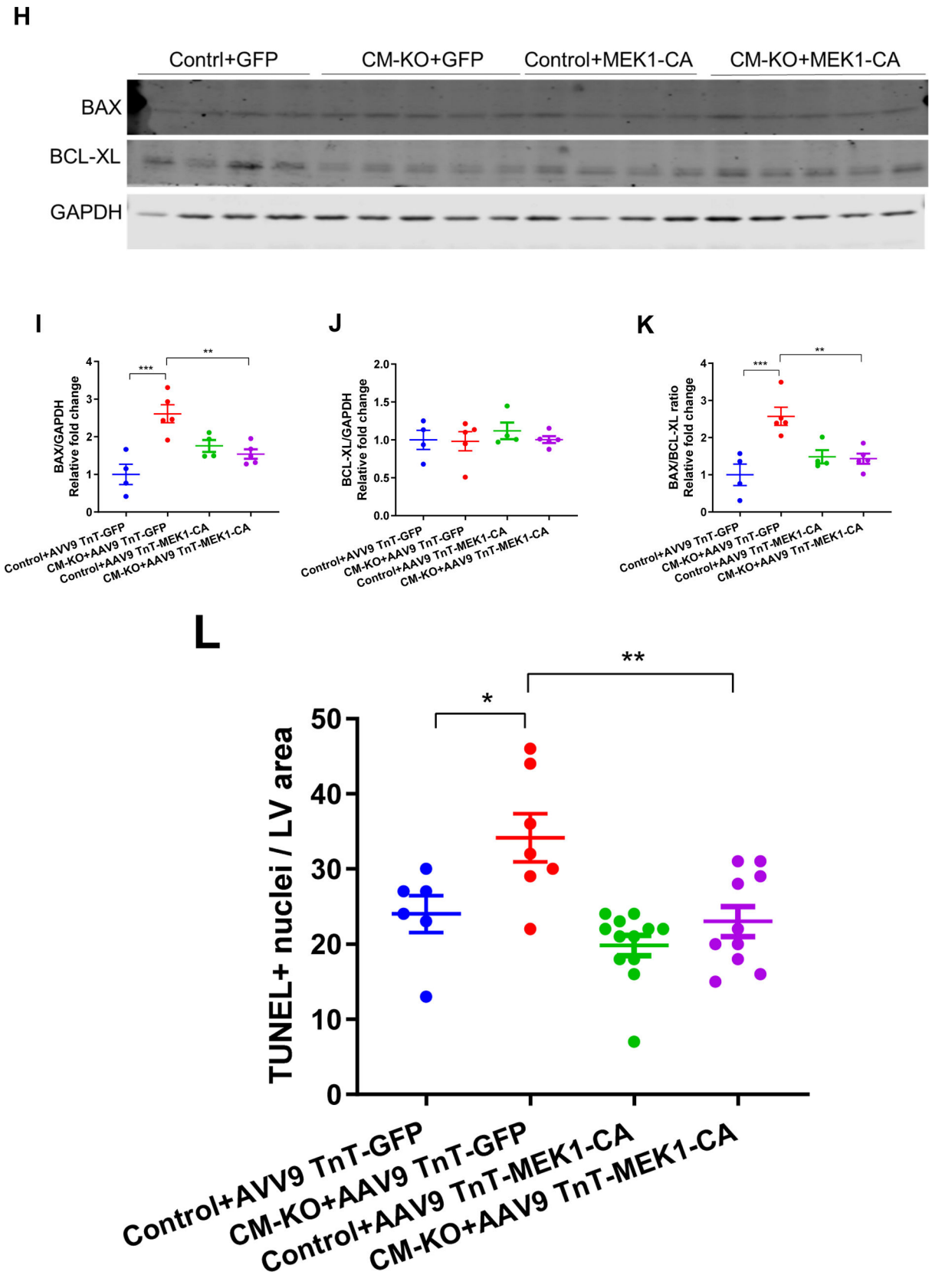

Figure 8. AAV9 TnT-MEK1-CA recues cardiac dysfunction in CM-KO. A.
The Map of the TnT-MEK1-CA plasmid used in our experiments for AAV9 packaging. **B**. Design of AAV9 rescue experiment. 1-month-old CM-KO or Control male mice were injected with either AAV9 TnT-GFP or AAV9 TnT-MEK1-CA via jugular vein. Echocardiography was performed before and after the injection at indicated time points to assess heart function. **C-E**. Protein expression of ERK phosphorylation, GFP and HA by Western blot. **C**. Representative immunoblot showing expression of p-ERK, t-ERK, GFP and HA. **D-E**. Quantification of ERK1 and ERK2 phosphorylation. Control+AAV9 TnT-GFP: n=4, CM-KO+AAV9 TnT-GFP: n=5, Control+AAV9 TnT-MEK1-CA: n=4, CM-KO +AAV9 TnT-MEK1-CA: n=5. **F-G**. Echocardiographic analysis of heart function of all experimental groups. **F**. Ejection fraction. **G**. Fractional shortening. Control+AAV9 TnT-GFP: n=7, CM-KO+AAV9 TnT-GFP: n=8, Control+AAV9 TnT-MEK1-CA: n=11–12, CM-KO+AAV9 TnT-MEK1-CA: n=9–10. *p<0.05 versus Control+AAV9 TnT-GFP, #p<0.05 versus CM-KO+AAV9 TnT-MEK1-CA, Mixed-effects analysis with Turkey's test. **H-K**. Protein expression of regulators in apoptotic pathway were measured with Western blot. **H**. Representative immunoblot showing expression of BCL-XL and BAX. **I-K**. Quantification of BAX, BCL-XL expression, and BAX/BCL-XL ratio in the CM-KO and Control LV. Control+AAV9 TnT-GFP: n=4, CM-KO+AAV9 TnT-GFP: n=5, Control+AAV9 TnT-MEK1-CA: n=4, CM-KO+AAV9 TnT-MEK1-CA: n=5. **L**. Quantification of TUNEL positive CM nuclei in the LV section. **p<0.01, *** p<0.005, one-way ANOVA with Turkey's post hoc test.